Agricultural and Forest Meteorology 178–179 (2013) 88–105

Contents lists available at SciVerse ScienceDirect

Agricultural and Forest Meteorology

journal homepage: www.elsevier.com/locate/agrformet

Measuring H_2O and CO_2 fluxes at field scales with scintillometry: Part II – Validation and application of 1-min flux estimates

B. Van Kesteren[a,*], O.K. Hartogensis[a], D. van Dinther[a], A.F. Moene[a], H.A.R. De Bruin[b], A.A.M. Holtslag[a]

[a] Wageningen University, PO Box 47, 6700 AA Wageningen, The Netherlands
[b] Freelance Consultant, Bilthoven, The Netherlands

ARTICLE INFO

Article history:
Received 30 March 2012
Received in revised form 23 January 2013
Accepted 25 January 2013

Keywords:
Canopy resistance
Eddy covariance
Light–response curves
Monin–Obukhov similarity theory
Penman–Monteith
Scintillometer

ABSTRACT

This paper evaluates four methods to obtain accurate averaged flux estimates under conditions of non-stationary turbulence. In Part I (Van Kesteren et al., 2012), we introduced and evaluated these four combined methods for 30-min averaging intervals, notably the flux-variance method, the Bowen-variance method, the structure-parameter method, and the energy-balance method. The aim of this paper, Part II, is to validate the accuracy of the 1-min flux estimates of the CO_2 flux, FCO_2, and the evapotranspiration/latent-heat flux, L_vE. Furthermore, we use the 1-min fluxes to investigate flux and vegetation responses under conditions of non-stationary turbulence. Using several validation methods, we show that both the eddy-covariance method and the energy-balance method are unsuitable for estimating fluxes over 1-min averaging intervals. The three other combined methods are more successful in determining 1-min fluxes. The random error is approximately half that of the eddy-covariance method, but still some issues limit the success. The Bowen-variance method has a +0.09 systematic error and moreover, 30% of the data had to be omitted, because the method requires more stringent conditions. Furthermore, the flux-variance method has a −0.15 systematic error. The structure-parameter method performs best of all methods and accurately resolves 1-min fluxes. With this method, we do a final validation with a different data set and show that also under dry conditions the method accurately resolves FCO_2, although L_vE was more difficult to resolve. In the last part, the structure-parameter method is successfully applied under conditions of non-stationary turbulence. We show that L_vE and FCO_2 have a different step response upon abrupt changes in solar radiation, because different processes drive these fluxes. Also, we observe a 2-min time lag between solar radiation and 1-min fluxes and show the relevance of taking this into account for determining light–response curves of the plants for both 1-min and 30-min averaging intervals. Furthermore, we show the relevance of 1-min fluxes for studying the light–response curves of plants for conditions with different temperature and humidity. Finally, we show that accurate estimates of 1-min averaged canopy resistances can be determined via the resistance expressions for sensible heat and L_vE. As such, we show that vegetation can indeed modify its canopy resistance significantly within several minutes.

1. Introduction

The eddy-covariance method is used worldwide for measuring evapotranspiration and CO_2 fluxes (Baldocchi, 2003; Shuttleworth, 2007). This method, which uses point-sampling measurements, typically determines fluxes on field scales (50–200 m). Furthermore, the eddy-covariance method obtains flux information over averaging intervals as short as 10 min, but typically 30–60 min (Hartogensis et al., 2002; Mahrt, 2010; Sun et al., 2005). During the averaging period, the turbulence is required to be stationary. This condition is violated for several common events such as rapidly changing cloud cover or intermittent turbulence.

Depending on the type, scintillometers estimate spatially averaged fluxes of momentum, sensible heat, and/or latent heat over distances varying from 100 m to 10,000 m. Confining ourselves to field scales (<500 m), it is important to note that the appropriate scintillometer, the displaced-beam laser scintillometer, can solely determine fluxes of sensible heat and momentum. Yet, literature shows that even over averaging intervals shorter than 1 min these scintillometer flux estimates are still accurate and when compared to eddy-covariance flux estimates also much more precise (Hartogensis et al., 2002; Wyngaard and Clifford, 1978). Consequently, this type of scintillometry does not require turbulence to be stationary over periods of 10–30 min. Scintillometer systems

* Corresponding author. Tel.: +31 317 483981; fax: +31 317 419000.
E-mail address: bram.van-kesteren@dwd.de (B. Van Kesteren).

0168-1923/$ – see front matter © 2013 Elsevier B.V. All rights reserved.
http://dx.doi.org/10.1016/j.agrformet.2013.01.010

that measure evapotranspiration on large scales (>1 km) are available (Evans, 2009; Green et al., 2001; Meijninger et al., 2006), but unfortunately these systems can neither be operated on field scales, i.e. over single crop fields, nor can they be used for measuring CO_2 fluxes, of fluxes of other passive scalars.

In Part I of this study (Van Kesteren et al., 2012), we introduced and validated four methods for averaging intervals of 30 min, which can determine evapotranspiration and other passive-scalar fluxes on field scales. They combine estimates of stability and friction velocity from the displaced-beam laser scintillometer with additional turbulence measurements of humidity or CO_2 to estimate the fluxes. These combined methods are called the flux-variance method (FVM), the Bowen-variance method (BVM), the structure-parameter method (SPM), and the energy-balance method (EBM).

The aim of this part (Part II) is to apply the spatial-averaging advantages of scintillometry to the four combined methods, so to evaluate evapotranspiration and CO_2 fluxes over short averaging intervals (~1 min). Therefore homogeneous conditions are required, which is ensured by limiting the application of the methods to single crop fields. The motivation to explore these relatively short flux-averaging intervals is that it provides us with a detailed mass-flux description in non-stationary circumstances. Consequently, with methods that can measure 1-min fluxes, turbulent exchange of vegetation with the atmosphere can be studied under natural, often non-stationary conditions (e.g. Foken et al., 2001). Furthermore, detailed, short-interval mass fluxes will teach us about plant behaviour in a natural environment and thus add to the highly controlled laboratory experiments that are usually performed on plants (e.g. Cardon et al., 1994). Moreover, by reducing the averaging time the flux comparison with snap-shot remote-sensing estimates can be improved. This improvement can especially be achieved in non-stationary conditions, when the snapshot of the satellite does not represent the 15–30 min flux data (Bastiaanssen et al., 1997). A similar argument holds for the validation and performance of hydrological/meteorological models. Models with fine horizontal or vertical resolution need to be operated with small time steps in order to keep the models stable. At present, these models are confronted with 15–30 min averaged fluxes, which partly conceal the qualities of/uncertainties in the models.

This paper elaborates on Part I and explores the possibilities of studying evapotranspiration, presented in terms of latent heat, and the CO_2 flux on time intervals as short as 1 min. At present, there are no direct flux-validation methods for 1-min averaging intervals. So to evaluate the performance of the combined methods on these short averaging intervals, we will follow two alternative approaches. First, we will test the accuracy of the 1-min flux estimates with an extensive error analysis. The error analysis is based on the error concepts of Lenschow et al. (1994), who show that the estimated fluxes differ systematically and randomly from the "ideal" ensemble average of a flux, when the averaging time is insufficient. We will determine these random and systematic errors for averaging intervals varying from 1 to 30 min. Second, we will estimate the accuracy of the 1-min averaged flux estimates by evaluating their reaction to rapid changes in the forcings of the fluxes. Net radiation is the energy available for the latent-heat flux and therefore is suitable to serve as a reference variable. In theory, the Penman–Monteith model (Monteith, 1965) would be the ideal validation method. However, in practice this model is limited because it assumes a closed energy balance, and requires an accurate description of the canopy resistance and of the roughness length for heat. Nevertheless, the Penman–Monteith model still is a more comprehensive validation method than net radiation. For the CO_2 flux, the incoming short-wave radiation will be used as a reference. The real forcing of FCO_2 is the photosynthetically active radiation (PAR), but the incoming short-wave radiation or solar irradiance is closely related to it (Papaioannou et al., 1993). Furthermore, for the structure-parameter method, estimates of both FCO_2 and L_vE will be validated for a wetter dataset than that of Transregio 2009 (i.e. Transregio 2008) and a dryer dataset (i.e. LITFASS 2009). As such, we investigate the accuracy of the method for conditions during which the similarity of sensible heat or humidity/CO_2 can break down (Andreas et al., 1998; De Bruin and Jacobs, 1993; De Bruin and Verhoef, 1999; Moene and Schüttemeyer, 2008).

One more aspect needs to be considered in the validation. Andreas et al. (2003) question the averaging advantage of scintillometers over point-sampling measurement techniques and the applicability of Monin–Obukhov similarity functions on short averaging intervals. Wyngaard and Clifford (1978) and Hartogensis et al. (2002) show that scintillometers do have an averaging advantage over point-sampling measurement techniques. Nevertheless, in the error analysis we will address both questions of Andreas et al. (2003) and show that accurate estimates of the flux can be obtained, even over short averaging intervals.

After the validation of the combined methods, we will discuss four applications for which the 1-min-flux measurements are necessary in Chapter 5. Firstly, we address the question what does changes on these short time intervals. Does the turbulence change (the transport mechanism) or does the vegetation affect the fluxes?

Secondly, studies of Foken et al. (2001) and Mauder et al. (2007) show that the sensible-heat flux, H, L_vE, and FCO_2 exhibit different time and amplitude responses to a decrease in solar radiation during a solar eclipse. They use wavelet analysis to investigate the fluxes, assuming that the high-frequency part of the turbulence spectrum dominates the fluxes. However, the two studies disagree with each other regarding the response times of the different fluxes. We will use our 1-min methodology and discuss the flux behaviour upon an instantaneous decrease in solar radiation caused by passing clouds. This discussion will be based on the different processes that govern these three fluxes.

Thirdly, we discuss light–response curves and the relevance of 1-min averaging values in determining these curves. Wolf et al. (2008) shows how the light–response curves can be used as a screening technique for erroneous data. Furthermore, light–response curves depend on atmospheric conditions such as temperature and humidity (Kim and Verma, 1990; Nieveen et al., 1998). Based on these notions, we will show the relevance of 1-min FCO_2 estimates for determining accurate light–response curves during conditions of non-stationary turbulence and their relevance for the comparison of light–response curves that are obtained during different atmospheric conditions.

Fourthly, we will discuss two methods for determining canopy resistances for 1-min averaging intervals. These methods are the Penman–Monteith method and the method using resistance expressions for H and L_vE (Baldocchi, 1994a; de Rooy and Holtslag, 1999; Moene and Van Dam, 2012; Nieveen, 1999). Based on the 1-min averaged canopy resistance, we will discuss the accuracy of both methods and study the response of plants to changes in radiation (cloud cover) and humidity during non-stationary conditions. In addition, we also discuss the question whether vegetation (in our case winter wheat) physiologically can react as fast as 1 min to changes in external forcings.

2. Theory and methods

2.1. Eddy covariance and scintillometry

The eddy-covariance method estimates the flux from high-frequency measurements of vertical wind speed and scalar concentration. Scintillometers determine the friction velocity and sensible-heat flux via turbulence induced scattering of their beams,

using wave-propagation theory and Monin–Obukhov Similarity theory (Van Kesteren et al., 2012). In the introduction, we argued that scintillometers perform better than the eddy-covariance method in estimating the ensemble-averaged fluxes over shorter averaging intervals. There are two reasons for this. First, contrary to the eddy-covariance method, scintillometers do not need to capture all flux-transporting scales of the co-spectrum of scalar and vertical wind speed. The displaced-beam laser scintillometer only observes eddies that are of similar size as its first Fresnel zone (for the current set-up ~9 mm). Turbulence theory describes how these eddies relate to the other eddies in the turbulence spectrum (Hartogensis et al., 2002; Thiermann and Grassl, 1992; Van Kesteren et al., 2012). Second, the number of independent samples per unit time observed by the scintillometer is larger than that of a point-sampling measurement, because scintillometers average both over space and time, whereas the point-sampling measurements only average over time. Therefore, provided the conditions are homogenous, scintillometers require significantly less averaging time (only ~1%) than eddy-covariance systems for acquiring accurate measurements (Hartogensis et al., 2002; Wyngaard and Clifford, 1978) (cf. Section 4.1).

2.2. Combined methods

The displaced-beam laser scintillometer determines u_* and H, but not the fluxes of passive-scalar quantities such as the latent-heat flux, L_vE and the CO_2 flux, FCO_2. To extend the optical-scintillometer application to mass fluxes Van Kesteren et al. (2012) proposed four methods that combine scintillometer measurements with additional turbulence measurements of humidity or CO_2. These methods are called the flux-variance method, the Bowen-variance method, the structure-parameter method, and the energy-balance method. For a detailed description of the combined methods, we refer to Van Kesteren et al. (2012). Here, we only give an overview of the turbulent variables used in the methods (see Table 1).

2.3. Validation methods

It is a challenge to come up with a proper validation method for 1-min averaged fluxes. Direct methods that accurately measure L_vE or FCO_2 over 1-min averaging intervals are lacking. Here, we propose two methods to validate the combined methods. The first method uses error analysis for validation and the second method uses a reference variable for validation, i.e. net radiation. Both methods are described below.

Table 1
The turbulence variables of the scintillometer and additional measurements to calculate the flux with the four combined methods.

Method	Scintillometer measurements	Additional point-measurements
Bowen-variance	H	σ_T, σ_x, and r_{Tx}
Flux-variance	u_*[a] and L_O	σ_x
Structure-parameter	u_*[a] and L_O	C_{x^2}
Energy-balance	H	Q_{net} and G

[a] L_O is the Obukhov length, σ_T is the standard deviation of temperature, σ_x is the standard deviation of humidity or the CO_2 concentration, r_{Tx} is the correlation coefficient of temperature and humidity or temperature and CO_2, C_{x^2} is the structure parameter of humidity or CO_2 concentration, Q_{net} is the net radiation and G is the soil-heat flux.

2.3.1. Error analysis

Measurement errors are quality parameters that specify the accuracy of a measurement and consequently they can serve to validate the combined methods. The error analysis we apply uses the error concept of Lenschow et al. (1994), who show that the estimated fluxes differ systematically and randomly from the "ideal" ensemble average of a flux, when the averaging time of the flux is not "long enough". This error applies to statistical moments of any order, but for our application only second order moments are important, i.e. fluxes (covariance between vertical wind speed and a given variable) and variances (a covariance of a variable with itself).

Fig. 1 shows a theoretical time spectrum of a (co)variance. For the systematic error (Fig. 1a) insufficient averaging results in the exclusion of some larger relevant eddy scales from the record (as indicated by the hatched area in Fig. 1a). Consequently, the (co)variance is systematically underestimated. For the random error (Fig. 1b) insufficient averaging results in too few independent samples to accurately determine the spectral intensity (the uncertainty is indicated by the thin lines). Consequently, the (co)variance has a random error.

2.3.1.1. Systematic errors. To determine the systematic error in L_vE and FCO_2 from the combined methods and eddy-covariance method, we use an averaging method similar to Sun et al. (2005). This method gives an estimate of the systematic error by comparing 30-min arithmetic means from the flux with averaging intervals shorter than 30 min to their corresponding flux with 30-min averaging interval. We introduce the relative systematic error

$$SE_i = \frac{\overline{x_i}^{30}}{x_{30}} - 1, \quad (1)$$

where SE_i is the systematic error for a given averaging interval i, x_i is the flux with averaging interval i (i = 1, 2, 3, 4, 6, 20, or 15 min), x_{30} is the flux with 30-min averaging interval, and $\overline{x_i}^{30}$ the 30-min

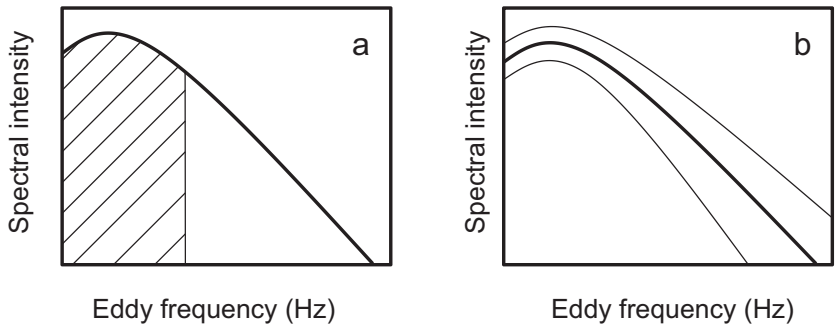

Fig. 1. Theoretical spectrum to indicate (a) the systematic error and (b) the random error. The errors occur, because in both cases the averaging time is insufficient. For the systematic error this results in missing large eddies (the hatched area) and an underestimation of the (co)variance. For the random error this results in having too few independent samples and a larger uncertainty (thin lines). All figure axes are logarithmic.

arithmetic mean of 30/i x_is. From rewriting Eq. (1) to $\overline{x_i}^{30} = (SE_i + 1)x_{30}$, it follows that the relative systematic error can be obtained from the regression slope of x_{30} with their corresponding $\overline{x_i}^{30}$.

The method described above considers discrete averaging intervals. A comparable, but continuous approach is the Ogive technique (Foken et al., 2006; Oncley et al., 1996). An Ogive is a cumulative integral of a time (co)spectrum and can be used for studying the systematic error in a (co)variance as a function of the continuous averaging interval. This follows from the fact that the integral of a (co)spectrum equals the (co)variance (Stull, 1988). With the Ogive approach, the systematic error is defined as

$$SE_i = \frac{\int_{\infty}^{f_{av}} Sdf}{\int_{\infty}^{f_{30}} Sdf} - 1, \tag{2}$$

where S denotes the (co)spectrum, f is the frequency, f_{av} is the frequency corresponding to a given averaging interval $f_{av} = 1/T_{av}$, and f_{30} is the frequency corresponding to an averaging interval of 30 min.

The Ogive approach cannot be used for determining the systematic error in the flux determined with the combined methods. However, the approach can be used for determining the systematic error in the (co)variances that serve as additional measurements for the combined methods (Table 1). For most input variables the application of the Ogive technique is obvious, but for the structure parameter, C_{x^2} it is not. In the following, we will therefore explain more about C_{x^2}.

C_{x^2}, is a spatial statistic, denoting fluctuations between two fixed points in space, and relates to the structure function by (Tatarskii, 1961)

$$C_{x^2} = D_{x^2} r^{-2/3} = \overline{[x(y) - x(y+r)]^2} r^{-2/3}, \tag{3}$$

where D_{x^2} is the structure function of quantity x, $\Delta x = x(y) - x(y+r)$ is the difference in concentration between position y and $y+r$, and the over-bar represents an average over the averaging time, T_{av}. The structure parameter can be determined from one time series by using Taylor's frozen turbulence approximation, so that $r = U\Delta t$, with U the mean wind speed and Δt the time difference between two measurements. When applying Reynolds decomposition to Eq. (3) it is important to realize that if $T_{av} \gg U\Delta t$, i.e. when the assumption of local isotropy holds, then $\overline{x(Ut)} = \overline{x(Ut + U\Delta t)}$. In that case, D_{x^2} for a given r can be written as

$$D_{x^2} = \overline{[x(Ut) - x(Ut + U\Delta t)]^2} = \overline{\left[x(Ut)' - x(Ut + U\Delta t)'\right]^2} = \overline{\left[\Delta x(Ut)'\right]^2}, \tag{4}$$

where Δx now denotes the temporal difference in quantity x. To understand the application of the Ogive technique to C_{x^2}, it is important to note that $\overline{\left[\Delta x(Ut)'\right]^2}$ is the variance of Δx. Therefore, applying the Ogive technique on Δx is to D_{x^2} and hence C_{x^2}, as applying the Ogive technique on x is to σ_x. This will allow us to determine also the systematic error of C_{x^2}.

2.3.1.2. Random errors. To determine the random error in L_vE and FCO_2 from the combined methods and eddy-covariance method, we use a method that considers discrete intervals. This method gives an estimate of the random error, by determining the fluctuations in the flux with averaging intervals shorter than 30 min normalized to their corresponding 30-min arithmetic mean. By normalizing to the 30-min arithmetic mean, we avoid the influence of the systematic error on the random error estimate. The random error is determined for cloud free conditions only. As long as the plants are not stressed and the stomata fully open, we can expect L_vE and FCO_2 (and also H) to closely follow the sine pattern of the diurnal cycle, so that any observed fluctuation can be attributed to the random error. We introduce the relative random error

$$RE_i = \sqrt{\frac{1}{N}\sum_{i=1}^{N}\left(\frac{x_i}{\overline{x_i}^{30}} - 1\right)^2}, \tag{5}$$

where RE_i is the random error for a given averaging interval i, x_i is the flux with averaging time i, $\overline{x_i}^{30}$ the 30-min mean of 30/i x_is to normalize x_i, and N the number of flux samples.

With the combined methods, we calculate the flux from measured variables that each has a random error. These variables are $K_{x,meth}$, which is the turbulent exchange coefficient of the method, and the statistical scalar variable, st(x), which is σ_x for the Bowen-variance and flux-variance methods, and C_{x^2} for the structure parameter method (Van Kesteren et al., 2012). The relative random error in the flux, F, is determined by the relative random error in $K_{x,meth}$ and st(x) as

$$\frac{\Delta F}{|F|} = \sqrt{\left(\frac{\Delta K_{x,meth}}{|K_{x,meth}|}\right)^2 + \left(0.5\frac{\Delta st(x)}{|st(x)|}\right)^2} \tag{6}$$

For the energy-balance method, absolute errors need to be considered. The absolute error in L_vE is determined by the absolute errors in Q_{net}, H and G through

$$\Delta L_vE = \Delta Q_{net} - \Delta H - \Delta G. \tag{7}$$

We want to reduce the random error in the flux by using the highly accurate measurements of the scintillometer, which define $K_{x,meth}$ in Eq. (6) and H in Eq. (7). In Section 4.1.2, we discuss the effects of the errors in the measurements on the random error in the flux.

2.3.2. Radiative forcing

The second validation method is a validation based on the net radiation, Q_{net}, and the incoming short-wave radiation, Q_s. Over well watered crops, fully covering the soil, Q_{net} is the main variable driving L_vE (De Bruin, 1987; Priestley and Taylor, 1972), since under these conditions H and G are relatively small. For FCO_2, Q_s is the main forcing variable. FCO_2 is the difference between the photosynthesis and the respiration of a system, i.e. the net ecosystem exchange (Scanlon and Kustas, 2010). During daytime, photosynthesis is dominant. Photosynthesis, in turn, is driven by the photosynthetic active radiation, which is a part of Q_s and hence closely related to it (Papaioannou et al., 1993). The radiometers have a time response of typically 5–10 s and they can therefore accurately resolve variations in Q_{net} and Q_s with time scales of 1 min.

Thus, the radiation can be used as a reference for validating the 1-min fluxes from the combined methods. Neither Q_{net}, nor Q_s are absolute measure of L_vE or FCO_2, but they can be seen as a relative reference in the sense that changes in the radiation should be followed by changes in the flux, also on short, 1-min time scales. We will use the correlation coefficient of Q_{net} against L_vE and Q_s against FCO_2 to quantify the response of the flux to changes in the radiation.

The Penman–Monteith method is a more comprehensive model to approximate the fluctuations in L_vE compared to Q_{net}, because fluctuations in L_vE are not only determined by Q_{net}, but also by G, vegetation, and the water-vapour deficit (Monteith, 1965). The model is given by

$$L_vE_{PM} = \frac{s(Q_{net} - G)}{s + \gamma\left(1 + \frac{r_c}{r_a}\right)} + \frac{\frac{\rho c_p}{r_a}(\overline{e_{sat}} - \overline{e_a})}{s + \gamma\left(1 + \frac{r_c}{r_a}\right)}, \tag{8}$$

where s is the slope of the saturated water-vapour pressure curve, e_{sat} is the saturated water-vapour pressure for a given

temperature, e_a is the actual water-vapour pressure, γ is the psychrometric constant, r_a is the aerodynamic resistance, and r_c the canopy resistance. The water-vapour deficit is given by $\overline{e_{sat}} - \overline{e_a}$ and $r_a = [\ln(z_{eff}/z_{0\theta}) - \Psi(z_{eff}/L_O) + \Psi(z_{0\theta}/L_O)]/k_{kar}u_*$, with the Ψ-functions for heat from Businger–Dyer (Businger et al., 1971; Paulson, 1970) and $z_{0\theta}$ the roughness length of heat. $z_{0\theta}$ is estimated as 1/10 of the roughness length of momentum, which in turn is estimated as 1/8 of the vegetation height (Green et al., 1994).

The Penman–Monteith model provides a direct estimate of L_vE, but for our study where we look at 1-min L_vE estimates, it cannot be used as an absolute reference. Instead, we will use it only as a relative measure, as we did with Q_{net}. The reason why the model can only be used as relative measure of L_vE is that two assumptions embedded in the model are violated in this study. First, the model assumes the energy balance to close on H, G, and L_vE. However, in Part I we show a non-closure of 19% of the energy balance, because the photosynthetic energy related to the carbon-dioxide flux and storage terms that account for the height differences of the measurements are not taken into account (Van Kesteren et al., 2012). Moreover, these storage terms are not constant throughout the day, but can vary greatly. Second, the model requires a detailed description of the canopy resistance, r_c, and of the roughness length for heat. Especially the dynamic behaviour of r_c on 1-min time-scales is not well parameterised and we therefore used a constant value of 50 s m^{-1} (Kelliher et al., 1995).

2.4. Determining 1-min averaged values of the canopy resistance

The combined methods potentially offer a great opportunity to determine the canopy resistance, r_c, of plants for intervals as short as 1 min. This can be done via inversion of the Penman–Monteith model or via the resistance expressions for H and L_vE.

With measurements of L_vE, r_c can be derived from the inverted Penman–Monteith model (e.g. Baldocchi, 1994a; Nieveen, 1999). However, this method involves several assumptions, most importantly a closed energy balance. In Part I we showed that for 30-min averaging intervals the energy balance does not close when only H, L_vE, and G are taken into account (Van Kesteren et al., 2012). Hence, to obtain r_c with this method, the influence of the heat-storage changes on the L_vE estimate must be quantified. Partly, this can be circumvented by accounting for the phase differences between the different components of the energy balance (cf. Foken et al. (2001) who concludes that using the delayed L_vE better closes the energy balance). Furthermore, this method models the atmospheric resistance and for that requires an accurate estimate of $z_{0\theta}$, see Section 2.3.2.

The method that uses the resistance expressions for H and L_vE is more straightforward. Deriving r_c from these expressions requires more simple additional measurements as those that are required for the previous method. The resistance expressions for H and L_vE read (de Rooy and Holtslag, 1999; Moene and Van Dam, 2012):

$$H = -\rho c_p \frac{\overline{T}(z) - \overline{T_s}}{r_a} \tag{9}$$

$$L_vE = -\rho L_v \frac{\overline{q}(z) - \overline{q_{sat}}(T_s)}{r_a + r_c} \tag{10}$$

where $T(z)$ is the temperature at height z, $q(z)$ the humidity at height z, T_s the radiative-surface temperature, $q_{sat}(T_s)$ the saturated specific humidity for a given T_s, r_a the atmospheric resistance, and r_c the canopy resistance.

Eqs. (9) and (10) are based on the assumptions that the air within the stomatal cavity is saturated with water vapour at a temperature T_s (Zeiger et al., 1987) and that the canopy resistance is a resistance that governs the transport from within a hypothetic, big leaf representing the vegetation layer to the surface of that leaf (Moene and Van Dam, 2012). Hence, with measurements of T, T_s, q, the pressure, p, and accurate 1-min estimates of H and L_vE, r_c can be solved. Unfortunately, measurements of T_s were not available in our experiment, but we do have measurements of outgoing and incoming long-wave radiation available, so that T_s can be estimated using (de Rooy and Holtslag, 1999; Huband and Monteith, 1986)

$$L^{\uparrow} = \varepsilon_s \sigma T_s^4 + (1 - \varepsilon_s) L^{\downarrow} \tag{11}$$

where $L^{\uparrow}$ is the outgoing long-wave radiation, $L^{\downarrow}$ is the incoming long-wave radiation, ε_s is the surface emissivity, and σ (5.67×10^{-8} W m^{-2} K^{-1}) is the Stefan–Boltzmann constant. For a wheat field with a completely closed canopy that approaches the heading stage, as is the case for Transregio 2009, $\varepsilon_s = 0.98$ (Chen and Zhang, 1989; Huband and Monteith, 1986; Wittich, 1997).

3. Experimental set-up and data treatment

This section describes the three field experiments from which data are used in this paper and the way the data are processed. The first and main experiment used in this paper is the Transregio32 project in 2009 (Graf et al., 2010). The measurements took place in a field with winter-wheat near Merken, Germany (50°50′53.92″ N, 6°24′1.99″ E) between 7 May and 10 June 2009. The dimensions of the field were 350 m × 150 m. In the middle of the field, an eddy-covariance system, consisting of a CSAT3 sonic anemometer (Campbell Scientific, Logan, USA) and a LiCor7500 H_2O/CO_2 sensor (LiCor, Lincoln, USA), were installed 2.40 m above ground level. Approximately 20 m west of the eddy-covariance tower, we installed a displaced-beam laser scintillometer (SLS-20, Scintec, Rottenburg Germany) at exactly the same height as the eddy-covariance system, with the middle of the scintillometer path centred at the tower. The scintillometer was installed at 2.40 m above ground level as well and had a path length of 120 m. The effective height of the scintillometer linearly decreased from 2.11 m at the beginning of the experiment to 1.84 m at the end of the experiment, due to the growing crop. Long-wave and short-wave radiation were measured at 2 m height in the EC tower with a four component net-radiation meter, NR01 (Hukseflux, Delft, the Netherlands). During the measurement period, the average temperature was about 15 °C. The amount of precipitation was 60 mm. Furthermore, during daytime the Bowen ratio, β, was generally smaller than 0.6 and z/L_O typically varied between −0.4 and 0.1. Consequently, the winter wheat was well watered and green during the whole measurement period. The measurement error in u_* as noted by De Bruin et al. (2002) and Hartogensis et al. (2002) was accounted for. For more details about the other measurements and specific set-up features we refer to Part I of this study (Van Kesteren et al., 2012).

The second experiment presented in this paper is also part of the Transregio32 project. The measurements were performed near Merken (Germany), between 7 August and 30 September 2008 at a sugar-beet field (50°50′47.85″ N, 6°23′50.99″ E) (van Dinther, 2009). The set-up was identical to the set-up of the 2009 field experiment. The installation height of both the LiCor7500 H_2O/CO_2 sensor (LiCor, Lincoln, USA) and the scintillometer (SLS-20, Scintec, Rottenburg Germany) was 2.20 m above ground level. Long-wave radiation was measured with a two-component CG1 pyrgeometer (Kipp & Zonen, Delft, the Netherlands) and short-wave radiation was measured with a two-component CM11 pyranometer (Kipp & Zonen, Delft, the Netherlands). The sugar beets were fully grown and about 0.70 m tall. Estimating the displacement height as 2/3 of the crop height (Green et al., 1994), this results in a displacement height of 0.47 m and consequently an effective scintillometer height of 1.73 m. Rain was plentiful during this experiment and the Bowen ratio was typically smaller than 0.5. As for Transregio

2009, the measurement error in u_* was corrected by fitting u_{*SLS} to u_{*EC} for 30-min averaging intervals. This resulted in a correction of $u_{*corrected} = (u_{*SLS} - 0.14)/0.3$ (van Dinther, 2009).

The third experiment presented in this paper is part of the LITFASS-2009 campaign (Beyrich et al., 2012). The aim of this experiment was to study a number of assumptions in the scintillometer data processing and interpretation that still call for a thorough evaluation, in particular over heterogeneous terrain (Beyrich et al., 2012). The LITFASS-2009 field campaign took place around the Meteorological Observatory Lindenberg-Richard-Aßmann-Observatory of the German Meteorological Service (DWD) from 29 June 2009 until 24 July 2009. The experiment used in this paper took place over a triticale field (52°10′54.6″ N, 14°07′11.0″ E), with field dimensions of approximately 500 m × 400 m. The set-up of the experiment presented here was similar to the set-up of the two Transregio32 experiments. The installation height of the LiCor7500 H_2O/CO_2 sensor (LiCor, Lincoln, USA) was 2.90 m above ground level and the scintillometer (SLS-20, Scintec, Rottenburg Germany) was installed 3.15 m above ground level. Furthermore, the scintillometer path length was 110 m. Long-wave radiation was measured with a two-component CG1 pyrgeometer (Kipp & Zonen, Delft, the Netherlands) and short-wave radiation was measured with a two-component CM11 pyranometer (Kipp & Zonen, Delft, the Netherlands). Triticale is a hybrid of wheat (*Triti*cum) and rye (S*ecale*). The plants were full-grown (1.2 m) and entered the senescent phase at the beginning of the experiment. Hence, estimating the displacement height as 2/3 of the crop height, i.e. 0.8 m, the effective scintillometer height was estimated to be 2.35 m. While the triticale plants dried out during the experiment, the typical Bowen ratio increased from 0.9 at the beginning of the experiment to 4.0 at the end of the experiment. The scintillometer u_* was corrected for its measurement error in the same way as it was done for the Transregio 2009 data (wheat), as these experiments took place right after each other and we used the same SLS-20.

All data were processed in the same way as described in Part I of this study (Van Kesteren et al., 2012), with two differences. Firstly, the eddy-covariance data were processed using the processing package ECpack from Wageningen University (Van Dijk et al., 2004), for averaging intervals of 1, 2, 3, 4, 6, 20, 15, and 30 min. Secondly, the scintillometer measurements were processed for the same averaging intervals.

The data for the validation with the error analysis is obtained in the following way. To estimate the relative systematic error, we first determine $\overline{x_i}^{30}$ and x_{30} for each half hour in the data set and subsequently apply linear-regression analysis to determine the regression slope (forced through origin and with a confidence interval of 95%). In addition, the root-mean-squared error (RMSE) of the regression is determined to indicate the accuracy of the error estimate. The larger the RMSE, the less representative the slope is for the systematic error.

To determine the systematic error with the Ogive technique, we used the raw, high-frequency eddy-covariance data to which no corrections have been applied yet. Therefore, we corrected these data for the humidity influence on sonic temperature in order to determine the specific humidity from the absolute humidity (Schotanus et al., 1983). Other corrections were not applied, because they only affect the small scales (high frequencies) or wind measurements. This is an adequate approach, because small scale errors cancel out when considering the relative errors and for the wind we only need an estimate of its mean value. Furthermore, these corrected data were divided in data blocks of 4 h instead of 30 min, to improve the estimate of the spectral intensity at 30 min (Foken et al., 2006). Finally, we determined the systematic error for all 4-h blocks in the whole data set.

To estimate the relative random error, we determine $\overline{x_i}^{30}$ and x_i for all cloudless conditions. $\overline{x_i}^{30}$ is determined such that the corresponding x_i is located at the centre of this 30-min interval. Furthermore, for this analysis data were omitted when L_vE of the method in question was lower than 30 W m^{-2} or for FCO_2 when $|FCO_2| > 0.5$ mg m^{-2} s^{-1}.

The data for the validation with the Penman–Monteith model is obtained in the following way. This validation is done for the complete data set. To avoid the situation that the diurnal cycle primarily determines the regressions statistics, we divide the data set into periods of 2 h and omit some of the data. Data are omitted when Q_{net} was not affected by clouds during a period of 2 h, when $L_vE_{PM} < 10$ W m^{-2}, or when for a 2-h period 60% or more of its data is missing. For the remaining data, we determine the correlation and RMSE over each 2-h period. Subsequently, the correlations and RMSEs obtained from the 2-h periods are averaged in order to get one value for the whole data set.

4. Validation of the combined methods

In this section the validation results of the combined methods are presented for 1-min averaging intervals. The aim of this section is to discuss the capability of the methods to accurately represent the 1-min fluxes of L_vE and FCO_2. In Section 4.1, we will start the discussion with an error analysis, followed by a discussion that is based on the radiative forcing in Section 4.2.

4.1. Validating the combined methods by means of error analysis

Lenschow et al. (1994) showed that insufficient averaging results in an averaging-time-dependent systematic error (underestimation) because of missing larger eddies and a random error (uncertainty) because of having too few independent samples. In Sections 4.1 and 4.2, we show the results of an error analysis to investigate how well each method approaches the ensemble averaged flux, as estimated by its 30-min averaged flux, for short averaging intervals. Note, that these 30-min averaged fluxes can still have systematic and random errors for other reasons than insufficient averaging. These errors were discussed in Part I and will not further be considered here.

4.1.1. Systematic errors

This section shows the results of the systematic error analysis. Firstly, the results of the systematic error in L_vE are shown for all methods. The results for FCO_2 are not shown, except for some results in Table 2, because they are very similar to those of L_vE (Van Kesteren, 2012). Subsequently, it is discussed that the methods achieve their accuracy by using scintillometer (scinti) estimates of H, u_* and L_O instead of eddy-covariance (EC) estimates of H, u_* and L_O. Building on that conclusion, we discuss each method individually and show to what extent the additional point-source measurements (Table 1) are of importance as well for estimating the ensemble averaged flux accurately. Finally, we discuss the applicability of Monin–Obukhov Similarity Theory on 1-min averaging intervals.

We start with Fig. 2, which shows the systematic errors in L_vE estimated with the combined methods, as a function of averaging time. The combined methods in Fig. 2a use H_{EC}, u_{*EC}, and $L_{O,EC}$ as "scintillometer" input, whereas in Fig. 2b they use H_{scinti}, $u_{*scinti}$, and $L_{O,scinti}$ (for input variables used per method, see Table 1). L_vE_{EC} is added as a reference and is identical in both subfigures. The systematic error estimates of the eddy-covariance system are based on ~350 h of data, whereas those of the scintillometer are based on only ~150 h of data, because of instrument malfunctioning during two weeks of the measurement campaign. In addition, the systematic errors in both L_vE and FCO_2 for 1-min averages are shown in Table 2 together with the RMSE of the regression analysis that is

Table 2
Systematic errors (SE) in L_vE, FCO_2, H, and u_* for 1-min averaging intervals. In addition, the root-mean squared error (RMSE) is given to indicate the accuracy of the error estimate. The fluxes are determined with different methods (see text) and when the combined methods are applied the fluxes are either calculated with sonic-anemometer data or scintillometer data. All regression statistics are based on a 95% confidence interval. Shorthand notations of the methods are the same as in Fig. 2.

	Sonic-anemometer data (EC)				Scintillometer data (scinti)			
	SE (−)		RMSE		*SE* (−)		RMSE	
	L_vE	FCO_2	L_vE	FCO_2	L_vE	FCO_2	L_vE	FCO_2
$Flux_{BVM}$	−0.10	−0.06	5 W m^{-2}	1.4×10^{-1} mg m^{-2} s^{-1}	+0.05	+0.09	7 W m^{-2}	1.1×10^{-1} mg m^{-2} s^{-1}
$Flux_{FVM}$	−0.26	−0.24	15 W m^{-2}	1.1×10^{-1} mg m^{-2} s^{-1}	−0.16	−0.16	7 W m^{-2}	7.3×10^{-2} mg m^{-2} s^{-1}
$Flux_{SPM}$	−0.08	−0.08	5 W m^{-2}	4.7×10^{-2} mg m^{-2} s^{-1}	+0.02	+0.02	2 W m^{-2}	3.1×10^{-2} mg m^{-2} s^{-1}
$Flux_{EBM}$	+0.02		4 W m^{-2}		0.00		2 W m^{-2}	
$Flux_{EC}$	−0.13	−0.12	10 W m^{-2}	7.6×10^{-2} mg m^{-2} s^{-1}				
H	−0.21		7 W m^{-2}		+0.01		2 W m^{-2}	
u_*	−0.08		1.6×10^{-2} m s^{-1}		+0.02		0.6×10^{-2} m s^{-1}	

used to quantify uncertainty in the mean-error estimate. Furthermore, the table shows the systematic error and the corresponding RMSE for the reference method and the "scintillometer" input variables, i.e. L_vE_{EC}, H_{EC}, H_{scinti}, u_{*EC}, and $u_{*scinti}$.

Before considering each method specifically, we will first look at two general issues of Fig. 2. First, note that the systematic errors for some of the combined methods are positive, i.e. $\overline{L_vE_{1\,min}}^{30}$ overestimates L_vE_{30min}. This counterintuitive overestimation is related to the fact that in the Bowen-variance method σ_T is inversely related to L_vE, as is H in the energy-balance method, and as is l_0 (through u_*) in the structure-parameter method.

Another issue that plays a role is that u_* non-linearly depends on l_0 by a −4/3 power, see Eq. (4) in Part I. As a result, in determining a 30-min interval u_*, u_* based on 1-min l_0 will be larger than u_* based on 30-min l_0, i.e. $\overline{u_*(l_{0,1\,min})}^{30} > u_*(l_{0,30\,min})$. This effect is enhanced due to the log-normal distribution of l_0. As L_vE and H depend linearly on u_* they are affected in a similar way, i.e. $\overline{L_vE(l_{0,1\,min})}^{30} > L_vE(l_{0,30\,min})$ and $\overline{H(l_{0,1\,min})}^{30} > H(l_{0,30\,min})$.

Second, comparison of Fig. 2a with Fig. 2b shows that the scintillometer outperforms the eddy-covariance method and greatly benefits the accuracy of the L_vE estimate. The obvious reason is that the systematic errors found in the scintillometer H and u_* estimates are much lower than those in the eddy-covariance estimates. For the data considered in Fig. 2, the systematic errors in the scintillometer H and u_* are +0.01 and +0.02, whereas for the eddy-covariance system the errors are −0.21 and −0.08 respectively (see Table 2). The error of −0.21 we found in H_{EC} is particularly large, when compared to values found in the literature (Sun et al., 2005). The high accuracy of the scintillometer is in agreement with previous results of Hartogensis et al. (2002), who conclude that the scintillometer is "superior" to eddy-covariance flux estimates when using short averaging intervals.

With these conclusions in mind, we now proceed to discuss the results of the systematic error in L_vE for each combined method. We will focus on the 1-min averaging intervals, unless stated otherwise. As we wish to improve upon the results of the eddy-covariance method, this method serves as a reference. The error in eddy-covariance L_vE is −0.12, which is similar to the error in L_vE reported by Sun et al. (2005).

The energy-balance method is the combined method with the smallest systematic error. For this method, Q_{net} is the most significant input and the only turbulence variable that suffers from the averaging-time-dependent systematic error is H. This error in H results in a systemic error in L_vE of +0.02 when H_{EC} is used and a zero error when H_{scinti} is used.

The flux-variance and Bowen-variance method have larger systematic errors than the energy-balance method, i.e. −0.27 and −0.10 when H_{EC}, u_{*EC}, and $L_{O,EC}$ are used and −0.15 and +0.05 when H_{scinti}, $u_{*scinti}$, and $L_{O,scinti}$ are used. Unlike the systematic error in the energy-balance method, the systematic error in the flux-variance method and the Bowen-variance method are not eliminated by using the scintillometer. This happens, because the additional measurements of both these methods are σ_T and/or σ_q (Table 1), which suffer from a systematic error, see below. The flux-variance method only gets as accurate as the eddy-covariance method, whereas the Bowen-variance method seems to perform better. Ideally, when $r_{Tq} = 1$, the errors in σ_T and σ_q cancel out against each other, but unfortunately this is only partly the case in our experiment. Note, that for this method the error for FCO_2 is larger than that of L_vE (Table 2). Also when considering the curves of the other methods as depicted in Fig. 2, the results for FCO_2 are more in agreement

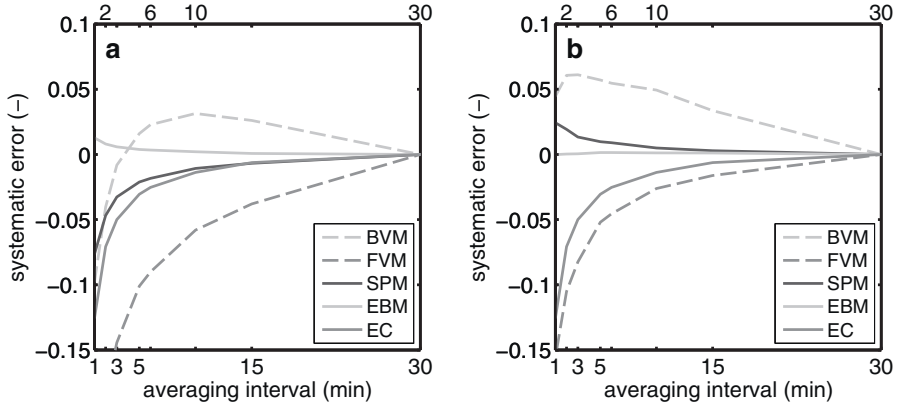

Fig. 2. Systematic measurement errors in L_vE related to averaging interval (a) using eddy-covariance data and (b) using scintillometer data. In the legend, BVM is the Bowen-variance method, FVM is the flux-variance method, SPM is the structure-parameter method, EBM is the energy-balance method, and EC is the eddy-covariance method.

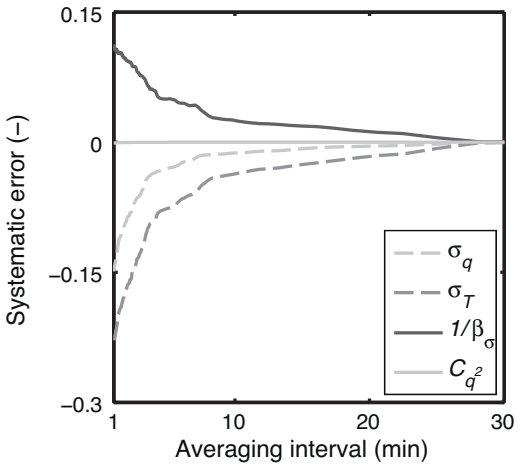

Fig. 3. Systematic error obtained with Ogive technique for the 23rd of May 2009 10:00 UTC–14:00 UTC.

with the other methods (not shown). Nevertheless, the differences between the error in FCO_2 and L_vE indicate the same – the errors in σ_T and σ_q or σ_{qCO_2} are not identical and do not cancel out against each other. Finally, the RMSE is low for these methods, yet larger than for the other two combined methods (Table 2). For both methods applies that the magnitude of the relative error for an individual interval can differ from the mean-error estimate and in case of the Bowen-variance method even can change sign sometimes (especially at night).

The structure-parameter method does improve upon the eddy-covariance method and the two variance-based methods. The systematic error in L_vE is virtually eliminated by using the scintillometer measurements. With the scintillometer H, u_*, and L_O the error is only +0.02 (RMSE = 2 W m^{-2}), which is brought about by the small systematic error in the scintillometer u_* and to a lesser extent by the small systematic error in L_O. Furthermore, the "additional variable" C_q^2 does not have a systematic error (see below).

To clarify how the errors in the additional variables propagate in the flux estimates, we will discuss the systematic errors in the additional variables of the combined methods. We determined the systematic errors, by applying the Ogive technique to high-frequency data of q, T, and Δq (Section 2.3.1.1). As such, we obtained the systematic errors for σ_q, σ_T, and C_q^2. Fig. 3 shows a representative example of the systematic error for these three variables during daytime. Also the systematic difference of the ratio of σ_q and σ_T, i.e. $\sigma_q/\sigma_T = 1/\beta_\sigma$, is shown, as this ratio directly shows how the errors in σ_q and σ_T propagate into L_vE for the Bowen-variance method. For the other methods, the relation between the structure parameter or variance and L_vE is direct.

For 1-min averaging intervals, the systematic error in σ_q is approximately −0.15, diminishing rapidly with increasing averaging interval, whereas the error in σ_T (−0.23) is larger and more persistent. Consequently, the systematic difference in $1/\beta_\sigma$ is positive and equals the difference between the error in σ_T and σ_q, i.e. a +0.10 error for 1 min averaging intervals. Apparently, σ_T, like H_{EC}, is influenced more strongly by larger time scales than σ_q, causing $|r_{Tq}| < 1$ and the error in $1/\beta_\sigma > 0$.

As σ_q and σ_T need a minimum averaging time (Fig. 1a) L_vE will always have a systematic error when estimated with the flux-variance method. Also, L_vE estimated with the Bowen-variance method will have a systematic error, except for "ideal" conditions when $|r_{Tq}| = 1$. However, often the conditions are not ideal. The structure-parameter method is a method that does not suffer from a systematic error, even when $|r_{Tq}| < 1$. C_q^2 is only defined for eddies of a size that falls in the inertial sub-range (Tatarskii, 1961) and is evaluated for one particular size, in our case 1 m. Simply because of how C_q^2 is defined, it is only sensitive to time scales corresponding to length scales of 1 m or smaller. Consequently, C_q^2 is insensitive to larger time scales, which are associated with the systematic error for variances (Fig. 1a).

Fig. 3 shows that, indeed, C_q^2 has no systematic error. Note, that the fact that the systematic error in C_q^2 equals zero for all averaging intervals does not imply that a 1-min averaged C_q^2 will correctly represent a 30-min averaged C_q^2. However, it does imply that taking the arithmetic mean of thirty 1-min averaged C_q^2 results in a correct estimate of the 30-min averaged C_q^2.

Moreover, with its high accuracy the structure-parameter method confirms that the application of Monin–Obukhov Similarity theory (MOST) is justified, even for these short averaging intervals. This contradicts the conclusion of Andreas et al. (2003), who argue that for non-stationary conditions 1-min averaged values of C_{n^2} and l_0 do not represent the 30-min averaged value of C_{n^2} and l_0. They base this argument on the observation that individual 1-min averages differ from the 30-min average. Then, they continue their argument in stating that because of the non-stationarity observed in the 1-min averaged fluxes, MOST functions, which are based on averaging intervals of 30–60 min may not be applied. However, 1-min averages may differ from 30-min averages. Essential for MOST is that for the dimensionless groups, y, $\overline{y_i}^{30} = y_{30}$, i.e. the ensemble average must be accurately estimated. Under homogeneous conditions, the scintillometer achieves this by a combination of spatial and temporal averaging, whereas the eddy-covariance method relies on temporal averaging only. Using spatial averaging to estimate the ensemble average is a technique that is also applied in large-eddy-simulation (LES) studies. In these studies it is standard practice to estimate the ensemble average at a given time by averaging over all grid points in homogeneous directions (e.g. horizontal slabs) (Cheinet and Siebesma, 2009). In contrast to LES models, a scintillometer always requires some temporal averaging as C_{n^2} is determined from a time-series of ln(I). However, the results above confirm that a 1-min averaging time is sufficient, since the scintillometer $\overline{u_{*1\,\mathrm{min}}}^{30} = u_{*30\,\mathrm{min}}$, $\overline{H_{1\,\mathrm{min}}}^{30} = H_{30\,\mathrm{min}}$ and for the structure-parameter method $\overline{L_vE_{1\,\mathrm{min}}}^{30} = L_vE_{30\,\mathrm{min}}$ and $\overline{FCO_{2,1\,\mathrm{min}}}^{30} = FCO_{2,30\,\mathrm{min}}$.

4.1.2. Random errors

Similarly to the previous section, we will evaluate the random error in L_vE_{EC} as well as in L_vE for all combined methods using the scintillometer- and the eddy-covariance H, u_* and L_O. Again, we will not show the results for FCO_2, because they are basically the same (Van Kesteren, 2012). We recall that we estimate the random error based on all cloudless data (520 samples). We will consider relative random errors and only use the 1-min averaging results in the discussion. The results are given in Fig. 4 and the random error in L_vE_{EC} (∼0.32) serves as the reference.

Comparing Fig. 4a with Fig. 4b shows that, as for the systematic error, using the scintillometer greatly reduces the random error in L_vE for all the combined methods that make use of additional turbulence humidity measurements. The random errors in the combined methods using H_{EC}, u_{*EC}, and $L_{O,EC}$ are ∼0.25 and these reduce to random errors of ∼0.17 when the combined methods are evaluated with H_{scinti}, $u_{*scinti}$, and $L_{O,scinti}$. The reason that the combined methods yield a smaller random error than the eddy-covariance method is twofold.

The first reason is that the scintillometer acquires more independent samples than the sonic anemometer, by sampling small eddies with the size of its first Fresnel zone (in this set-up ∼9 mm) (Wyngaard and Clifford, 1978). As a result the random error in $K_{q,meth}$ is greatly reduced, see Eq. (6). For the data shown in Fig. 4,

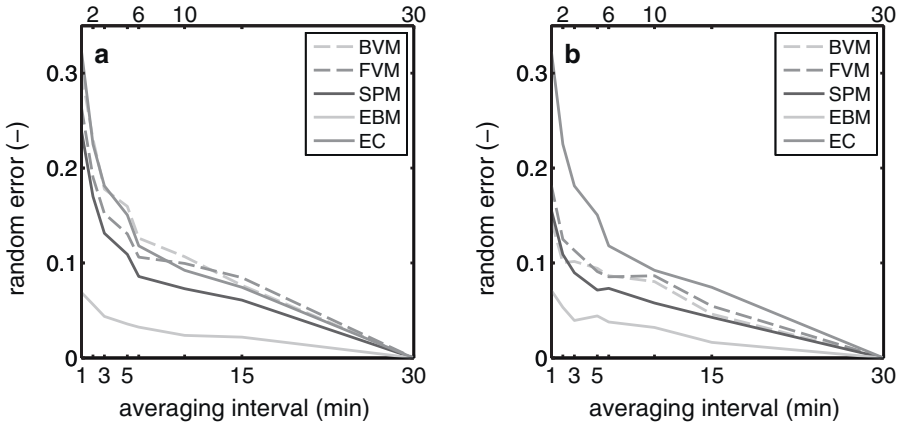

Fig. 4. Random measurement errors for L_vE related to averaging interval (a) using eddy-covariance data and (b) using scintillometer data. In the legend, BVM is the Bowen-variance method, FVM is the flux-variance method, SPM is the structure-parameter method, EBM is the energy-balance method, and EC is the eddy-covariance method.

the random error in e.g. scintillometer H is 0.11, whereas for the eddy-covariance system the error in H is 0.3. This is in line with Hartogensis et al. (2002), who found that the random error in H_{EC} was about twice the error in H_{scinti}.

The second reason is that the random error in the humidity variable is small. The error in L_vE for the combined methods is determined by the decorrelation time of q, whereas the error in L_vE_{EC} is determined by the decorrelation time of w. Two advantages follow from not using cov(w,q), but $\sqrt{\text{var}(q)}$ or $\sqrt{C_q^2}$. Firstly, Eq. (49) of Lenschow et al. (1994) shows that a low r_{wq} (in our case $r_{wq} \approx 0.3$) increases the time to acquire enough independent samples for a covariance as compared to a variance (in our case with a factor ten). Hence, as long as the decorrelation time of q is less than ten times longer than that of w, the resulting random error in var(q) still is smaller than that in cov(w,q). Secondly, using $\sqrt{\text{var}(q)}$ or $\sqrt{C_q^2}$ ensures that the relative error in var(q) or C_q^2 propagates with a factor 0.5 to L_vE, see Eq. (6). Thus, the net effect is that as long as the decorrelation time of q is less than twenty times larger than the decorrelation time of w, the random error in L_vE estimated with the combined methods is smaller than the random error in L_vE_{EC}. Even close to the surface, where the decorrelation time of w is much smaller than that of q this is guaranteed.

In the analysis above, the energy-balance method was not taken into account because its estimate of L_vE depends mostly on an accurate estimate of Q_{net}. As for the systematic error, the energy-balance method has the lowest random error of all methods. The random error in L_vE is about 0.06 for 1-min averaging intervals when estimated with this method. However, data were excluded for $L_vE < 70\ \text{W m}^{-2}$, otherwise the error was dominated by data from the transition from $Q_{net} > 0$ to $Q_{net} < 0$. If these data are included, the random error increases to 0.17. This increase happens, because during the transition time, H is large compared to L_vE and its magnitude is similar to the sum of Q_{net} and G. Consequently, even though the relative random error in H is small, the absolute random error is large compared to the small L_vE. The resulting relative random error in L_vE is relatively large, because the large absolute error in H propagates to L_vE, see Eq. (7).

4.2. Validating the combined methods by means of radiative forcing

In this section, we validate the combined methods by evaluating the errors in 1-min estimates of L_vE and FCO_2 with Q_{net} and Q_s respectively. For that, we single out two situations and evaluate L_vE with Q_{net}. In addition, we validate the data from the whole experiment with the Penman–Monteith model for L_vE. Finally, we do a last validation of the structure-parameter method under dryer and wetter conditions than those that occurred during the Transregio-2009 campaign. In the previous section we showed that the systematic and random errors of the combined methods using scintillometer H, u_*, and L_O outperform the eddy-covariance estimates of L_vE and FCO_2 for 1-min averaging intervals. From hereon we will therefore only apply the combined methods with the scintillometer H, u_*, and L_O.

4.2.1. Evaluating the combined methods with Q_{net} and Q_s

The evaluation of the combined methods with Q_{net} and Q_s is done by considering the correlation between Q_{net} and L_vE and Q_s and FCO_2 as described in Section 2.3.2. Fig. 5 shows the time series of 1-min averaged Q_{net} and L_vE between 7:00 and 12:00 UTC on 4 June 2009 with time steps of 1 min for all the combined methods and the eddy-covariance method. The figure depicts a situation during which cloudy and sunny spells rapidly succeed each other, so that Q_{net} fluctuates abundantly. Consequently, we expect L_vE to fluctuate as well. Note, that even though Q_{net} drives L_vE we do not expect a perfect correlation between the two variables, because the available energy (represented by Q_{net}) is not only distributed to L_vE, but also over other surface fluxes, and some energy is stored.

The first impression from Fig. 5 is that the eddy-covariance and Bowen-variance methods (Fig. 5a,b) perform worse than the flux-variance, structure-parameter, and energy-balance methods (Fig. 5c–e). In the following, we examine all five methods in detail.

Starting with the eddy-covariance method, we see many fluctuations in L_vE. The random error is so large that the radiation-driven fluctuations in L_vE tend to disappear in the random noise. The corresponding correlation with zero time lag, r_0, between L_vE and Q_{net} is 0.34. For the combined methods, we see that the Bowen-variance method correlates better with Q_{net} than was the case for the eddy-covariance method. However, 24% of data are missing, because data were omitted when $|r_{Tq}| < 0.2$ or $|\beta| < 0.1$ or in case of FCO_2 when $|r_{TqCO_2}| < 0.2$ or $|\alpha| < 1$ (α is the Bowen ratio for CO_2). The flux-variance method and structure parameter method perform better than the Bowen-variance method. They both resolve the variations in L_vE well, have a higher data availability, and r_0 is higher, i.e. 0.60 and 0.59 respectively.

Note that Fig. 5a–d besides r_0 also shows the correlation with 1 or 2 min time lag, r_1, r_2, i.e. the correlation of $Q_{net}(t)$ with $L_vE(t+1)$ or $L_vE(t+2)$. We determined the optimal time lag, so that r_{lag} is maximal. For all four methods, r_{lag} is significantly larger than r_0. All methods, except the Bowen-variance method ($r_1 = 0.59$ and $r_2 = 0.58$) agree with each other on the time lag of 2 min. Thus, it seems likely that the time-lag is about 2 min.

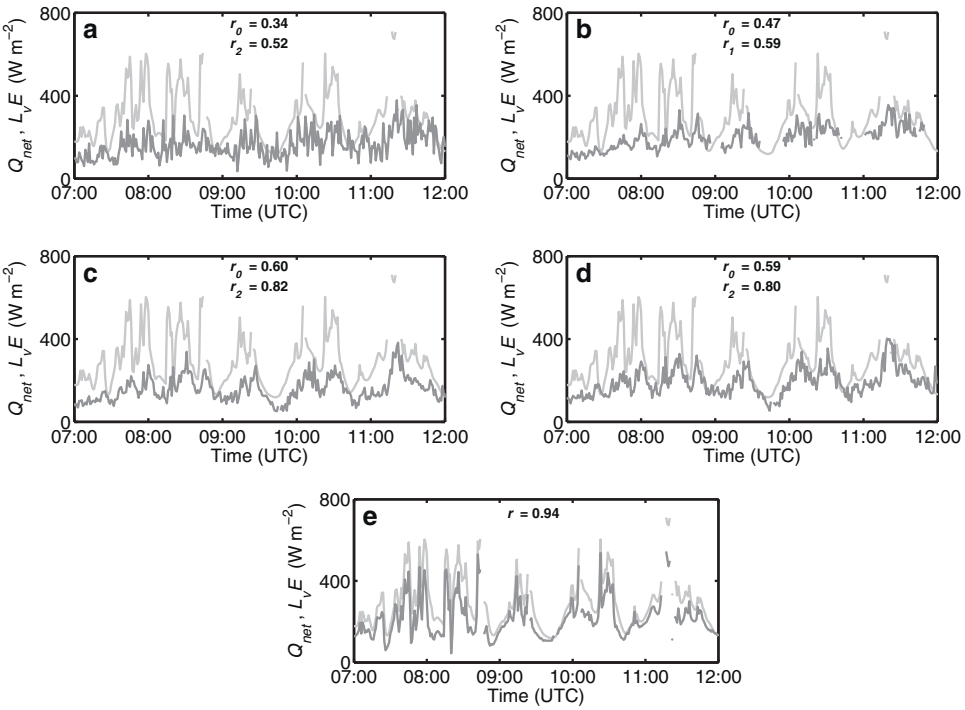

Fig. 5. 1-min L_vE and net radiation on 4 June 2009, (a) eddy-covariance method, (b) Bowen-variance method, (c) flux-variance method, (d) structure-parameter method, and (e) energy-balance method. In all graphs, r is the correlation coefficient of the net radiation (light grey) with L_vE (grey).

When considering the correlation between Q_s and FCO_2 a similar pattern is observed (not shown). Again, we do not expect a perfect correlation between the two variables, because Q_s does not exactly equal the photosynthetically active radiation and light saturation occurs for $Q_s > 300\,W\,m^{-2}$. Nevertheless, the correlation between Q_s and FCO_2 is larger than that was observed between Q_{net} and L_vE. For the eddy-covariance method $r_0 = 0.50$ and $r_2 = 0.65$, for the Bowen-variance method $r_0 = 0.66$ and $r_1 = 0.78$, for the flux-variance method $r_0 = 0.71$ and $r_2 = 0.89$, and for the structure-parameter method $r_0 = 0.72$ and $r_2 = 0.88$. From this we can conclude that also FCO_2 has a time lag of 2 min. The reason for the time lag of the fluxes is discussed in Section 5.2, here it suffices to say that it is related to the storage capacity of the system.

Finally, the energy-balance method is added for completeness. The energy-balance method clearly overestimates L_vE as a result of the non-closure of the energy balance (Van Kesteren et al., 2012). Furthermore, the phase of L_vE is biased to that of Q_{net}, which makes that the method is not capable of capturing the 2-min inertia of the system. More in general, Q_{net} is unsuitable as a validation method for the energy-balance method, because of the strong cross-correlation between method and reference through Q_{net}. This is especially true for the conditions encountered in this experiment, where H and G are relatively small compared to Q_{net} and the storage terms and the energy equivalent of the CO_2 flux are neglected. Therefore, the large correlation coefficient ($r = 0.94$) cannot be considered to be an indication of accuracy.

From the above result we can conclude that the assumption of a closed energy balance does not hold for 1-min averaging intervals. Consequently, we expect that the Penman–Monteith model, our second validation method, is affected by the invalidity of this assumption as well. In the following, we will discuss the accuracy of the energy-balance method and the Penman–Monteith model. Fig. 6 shows Q_{net} together with L_vE estimated with the energy-balance method, the Penman–Monteith model, and the structure-parameter method, which we added for comparison. Furthermore, we highlighted and numbered three events with distinct changes in radiation to guide the discussion.

From the error analysis and Q_{net} validation, we know that the structure-parameter method resolves L_vE accurately for each of these three events. As in Fig. 5, the abrupt changes in Q_{net} are

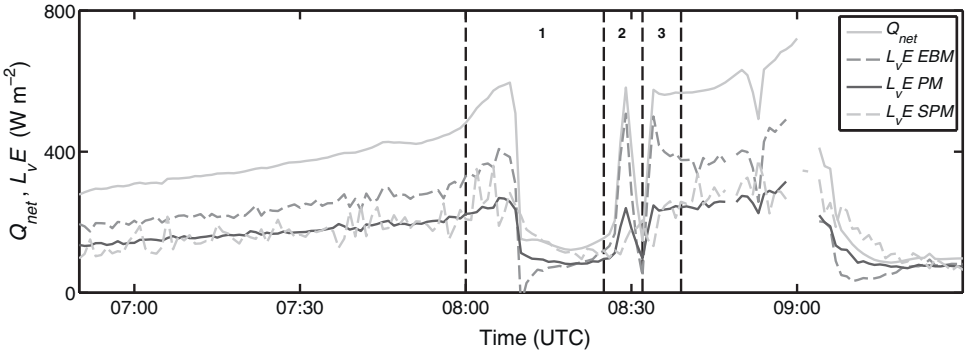

Fig. 6. Responses of L_vE to variable radiation, 5 June 2009 from 7:00 UTC to 10:30 UTC. L_vE with 1-min averaging intervals is shown for the energy-balance method, the Penman–Monteith model, and the structure-parameter method.

Table 3
Comparison of the combined methods and the eddy-covariance method with Penman–Monteith for 1-min averaging intervals of L_vE. Shown are: r, the correlation coefficient, RMSE, the root mean-square error, and n the total number of 1-min samples included in the calculations. Finally, the subscript 0 denotes a 0-min time lag and the subscript 2 denotes a 2-min time lag of L_vE.

	r_0 (−)	RMSE_0 (W m^{-2})	r_2 (−)	RMSE_2 (W m^{-2})	n (−)
Eddy-covariance	0.51	74	0.58	54	2302
Bowen-variance	0.71	38	0.72	34	1541
Flux-variance	0.72	41	0.76	31	2181
Structure-parameter	0.72	42	0.76	31	2181

followed by delayed and slightly damped (event 2) changes in L_vE. The energy-balance method and the Penman–Monteith model are not able to resolve this inertia.

Moreover, the energy-balance method response on changes in Q_{net} is extreme. During the first event, the method shortly estimates a negative L_vE, immediately followed by an increase in L_vE, even though Q_{net} remains constant. During the third event a similar thing happens, but now mirrored as compared to the first event. This is not a physical response of L_vE upon changing Q_{net}, but it reflects the inertia in H. Hence, given the local circumstances, we conclude that the energy-balance method is unsuitable for measuring 1-min averaged fluxes.

The Penman–Monteith model yields better L_vE estimates than the energy-balance method, but the phase of its L_vE estimate is biased to Q_{net} as well. Both the assumption of a closed energy balance and constant r_c contribute to this. Despite these limitations in our model set-up, the Penman–Monteith model still gives a more comprehensive approach to fluctuations in L_vE than Q_{net} only. Especially during the late afternoon and early night, when the second term in Eq. (8) (water-vapour demand) dominates over the first term (the radiation term), the model is an improvement on Q_{net}.

4.2.2. Validating the combined methods with Penman–Monteith

This section continues with the validation of the combined methods with the Penman–Monteith model based on data from the whole experiment. Table 3 shows the correlation coefficient and RMSE that resulted from the regression analysis. Both statistical parameters are shown without time lag and with a 2-min time lag.

For 30-min averaging intervals, the Penman–Monteith model compares to the eddy-covariance method with a regression slope of 0.96x, a correlation of 0.97 and a RMSE of 22 W m^{-2}. For 1-min averaging intervals, the eddy-covariance method compares worst of all methods. The method has the largest RMSE (RMSE_0 = 74 W m^{-2} and RMSE_2 = 54 W m^{-2}) and its correlation is the lowest (r_0 = 0.51 and r_2 = 0.58). Assuming a 2-min time lag, improves the comparison, but despite the improvement, we see that the eddy-covariance method is not able to resolve rapid fluctuations in L_vE. Together with the fact that the method has a large systematic error, this leads to the conclusion that the method is unsuitable for measuring 1-min averaged fluxes.

The three combined methods perform better than the eddy-covariance method. All three combined methods yield good results in resolving fluctuations in L_vE. The Bowen-variance method, however, misses 30% of the data. These data were omitted, because like De Bruin et al. (1999) we found that the Bowen-variance method produces unreliable results when $|r_{Tq}| < 0.2$ or $|\beta| < 0.1$. The flux-variance method resolves fluctuations in L_vE even slightly better than the Bowen-variance method (r_0 = 0.72 and r_2 = 0.76, and RMSE_0 = 41 W m^{-2} and RMSE_2 = 31 W m^{-2}). Nevertheless, the method is less suitable to measure 1-min averaged L_vE than the structure-parameter method, because of its large systematic error. The structure-parameter method resolves the fluctuations in L_vE well (r_0 = 0.72 and r_2 = 0.76, and RMSE_0 = 42 W m^{-2} and RMSE_2 = 31 W m^{-2}) and moreover, the method does neither suffer from a systematic error, nor misses 30% of its data. Therefore, we conclude that the structure-parameter is the best and most robust method to measure L_vE for 1-min averaging intervals. Consequently, in the following we will apply the structure-parameter method to extend the validation to conditions that were wetter and dryer than the conditions used for the previous validation.

4.2.3. Evaluating the structure-parameter method with Transregio2008 and LITFASS2009 data

In the previous sections we validated the combined methods for L_vE and FCO_2 with data from the Transregio2009 experiment. In this section, we will do a final validation in which we regard both L_vE and FCO_2. The data used in this section come from Transregio2008 and LITFASS2009, i.e. for sugar beets under relatively wet conditions and for triticale under relatively dry conditions.

Fig. 7 shows Q_{net} with L_vE (a) and Q_s with FCO_2 (b) over the sugar beets on the 14th of August 2008. Both fluxes show a comparable, high correlation with the radiation (r_1 = 0.84 and r_1 = 0.90 for L_vE and FCO_2 respectively). This is similar as to what was observed over the wheat field in the 2009 experiment (r_2 = 0.80 for L_vE and r_2 = 0.89 for FCO_2). Precipitation characterized the 2008 experiment and the conditions were wetter ($\beta \approx 0.2$) than during the 2009 experiment ($\beta \approx 0.3$). The optimal time lag for the correlation over the sugar beets is 1 min, which is 1 min faster than was observed over the wheat in the 2009 experiment. Probably this is related to the lower crop density of the sugar beets compared to the wheat. Wheat has a large crop density (in terms of dry and wet matter as well as leaf-area index) and the leafs and the stems form a dense canopy compared to the canopy of sugar beets. Consequently, less storage is possible in sugar beets than in the wheat.

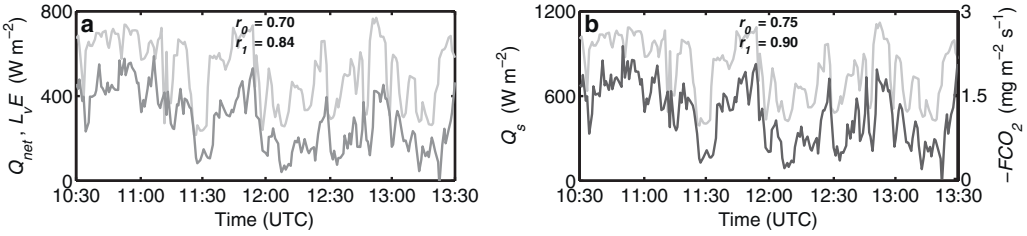

Fig. 7. Influence of (a) varying net radiation on L_vE and (b) incoming short-wave radiation on FCO_2 for a situation on 14 August 2008 from 10:30 UTC to 13:30 UTC. Measurements were made over sugar beets and the Bowen ratio was about 0.2. In (a) Q_{net} is light grey and L_vE is grey. In (b) Q_s is light grey and $-FCO_2$ is dark grey.

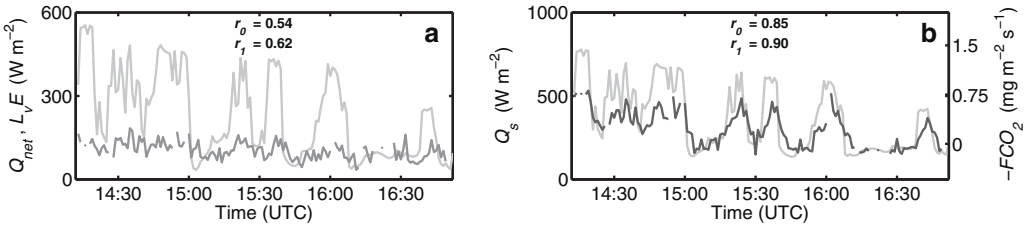

Fig. 8. Influence of (a) varying net radiation on L_vE and (b) incoming short-wave radiation on FCO_2 for a situation on 9 July 2009 from 14:00 UTC to 17:00 UTC. Measurements were made over triticale and the Bowen ratio varied between 0.3 and 2.5. In (a) Q_{net} is light grey and L_vE is grey. In (b) Q_s is light grey and $-FCO_2$ is dark grey.

Fig. 8 shows Q_{net} with L_vE (a) and Q_s with FCO_2 (b) over the triticale on the 9th of July 2009 during the LITFASS-2009 experiment. The triticale was in its senescence phase and slowly dried out during the experiment. Furthermore, the Bowen ratio fluctuated and reached values of about 2.5 during the sunny spells and 0.3 during the cloudy periods. These conditions are drier than during the two Transregio32 experiments. Just as for the sugar beets, the optimal time lag is 1 min. Triticale is a grain, as is wheat, but it has dried out and hence lost some of its storage capacity.

For L_vE, the correlation is clearly lower than in the previous experiments, $r_1 = 0.62$. Also when using the flux-variance method, $r_1 = 0.70$ (not shown). However, FCO_2 still has a large correlation with Q_s ($r_1 = 0.90$), even though FCO_2 is much smaller than in the previous two experiments (during the cloudy situations respiration dominates over photosynthesis). Also C_q^2 hardly correlates with Q_{net}, whereas $C_{qCO_2}^2$ does correlate with Q_s (not shown). Thus, it seems that in contrast to the CO_2 availability, the water availability is limited, causing the decorrelation of L_vE and Q_{net}. Note, that the different correlations do not indicate that L_vE and FCO_2 have become dissimilar (the combined methods assumes similarity). Similarity only concerns the way the scalars are transported through the atmosphere and it does not require the fluxes to be identical.

The above-mentioned results from the validations with the error analysis, the validation with Q_{net} and Q_s, both for Transregio2009 and the other experiments show a clear agreement between L_vE and FCO_2. FCO_2 and L_vE represent the surface fluxes of two passive scalars, water vapour and carbon dioxide. This leads us to the conclusion that the validation results of the combined methods generally holds for passive scalars.

5. Applications of 1-min evapotranspiration and CO_2 fluxes

In this section, we will apply the structure-parameter method to study flux responses and vegetation responses under non-stationary conditions. From here onward, we will use the Transregio-2009 data again (winter wheat) and consider 1-min averaging intervals. We will start with using the method to discuss the different responses of L_vE and FCO_2 upon decreased radiation (Sections 5.1 and 5.2). Then, we will discuss the relevance of determining light–response curves based on 1-min averaging intervals (Section 5.3). Finally, we will determine 1-min averaged canopy resistances and discuss plant behaviour for two days with significantly different atmospheric conditions (Section 5.4).

5.1. Plants versus turbulence

In this section, we investigate whether the fast response of L_vE to Q_{net} and FCO_2 to Q_s is brought about by a quick adaptation of turbulence or a quick adaptation of plants. To distinguish between the two, we recall the equation of the structure-parameter method for L_vE

$$L_vE = -L_v\rho u_* q_* = -\rho z^{1/3}\frac{L_v u_*}{\sqrt{f_q(z/L_O)}}\sqrt{C_{q^2}} = -\rho K_{q,strpar}\sqrt{C_{q^2}}, \quad (12)$$

where ρ is the density, $f_q(z/L_O)$ is a MOST function, and $K_{q,strpar}$ is the turbulence transport efficiency of the structure-parameter method. As z, L_v, and ρ are approximately constant in time, the most variation occurs in either C_q^2 or $K_{q,strpar}$. Here, we will discuss the response of L_vE, because it is representative for FCO_2 and other passive-scalar fluxes as well (not shown).

To check if the most variation occurs in C_q^2 or in $K_{q,strpar}$ we introduce Fig. 9, which shows Q_{net} together with C_q^2 and $K_{q,strpar}$ for the same situation as Fig. 6 on the 5th of June 2009. Fig. 9 shows that $K_{q,strpar}$ does not correlate with Q_{net}. Through L_O, $K_{q,strpar}$ is determined by u_* and H and of these two variables, Q_{net} directly influences only H. In Part I, we showed that the influence of H on $K_{q,strpar}$ (and thus on L_vE) is small, whereas the influence of u_* is relatively large (Van Kesteren et al., 2012). Furthermore, u_* is sensitive to the wind speed and to adapt to changes in Q_{net} during daytime takes about 25 min (Foken et al., 2001). Perhaps, in this specific case $K_{q,strpar}$ could also be obtained by interpolating 15-min or 30-min averaged eddy-covariance measurements. However, especially during conditions of changing wind speed, when buoyancy gets more important (during conditions of free convection), or during periods of intermittent turbulence this approach does not hold.

C_q^2, on the other hand, does strongly correlate with Q_{net}. C_q^2 is determined by the concentration above the sensor and below it. We assume that the concentration above the sensor remains constant, whereas the concentration below the sensors (close to the canopy) changes. This concentration changes either, because the vegetation closes its stomata or because the concentration within the stomatal cavity changes. In the following, we will investigate, which of the two possibilities occurs.

5.2. Exploring mechanisms that drive L_vE and FCO_2

The previous section shows that close to the surface, the flux forcings mainly affect the variations in humidity, but not the atmospheric turbulence, i.e. the transport mechanism. This is in line with findings in literature, which show various responses of the surface fluxes to changes in radiation (Foken et al., 2001; Mauder et al., 2007). In the following, we will use the 1-min fluxes to study the flux responses upon an almost instantaneous change in radiation (a step response). The 1-min fluxes enable us to do a detailed study of the flux response and discuss the mechanisms that cause L_vE and FCO_2 to respond differently upon changes in radiation.

To this end, we introduce Fig. 10, which compares L_vE and FCO_2 with Q_s for the same situation as the previous section. Fig. 10a shows Q_s with L_vE and $-FCO_2$ plotted such that they overlap and Fig. 10b shows Q_s with the ratio of $-FCO_2$ and E ($E = L_vE/L_v$). This

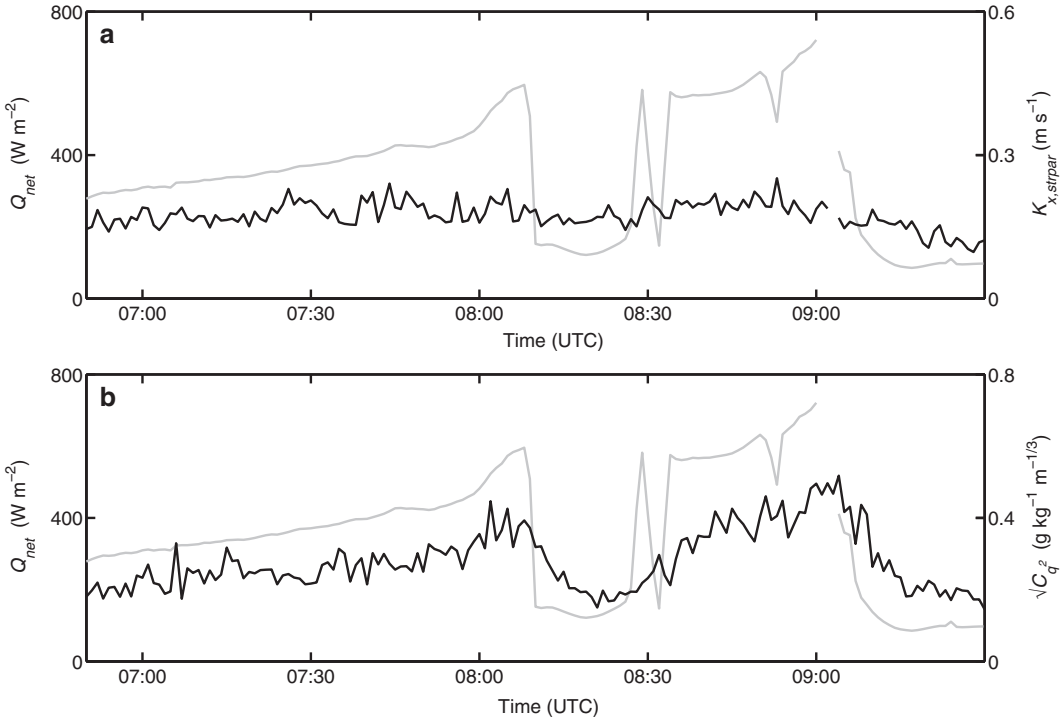

Fig. 9. Influence of varying net radiation. The grey line is the net radiation and the black line (a) the turbulent transport efficiency, and (b) the structure parameter.

ratio is similar to the water-use efficiency, with this difference that it is not corrected for the respiration flux (~0.3 mg m^{-2} s^{-1}), which is an order of magnitude smaller than the photosynthesis. Taking into account the low respiration rate and the fact the wheat is almost fully grown and fully covers the soil, it is feasible to assume that transpiration mainly determines L_vE and that photosynthesis mainly determines FCO_2 (cf. Scanlon and Kustas, 2010). Therefore, we will do so from hereon. Finally, three specific events are marked in order to guide the analysis.

During the first event, Q_s suddenly drops (8:08 UTC) and Fig. 10a shows that after 8:10 UTC FCO_2 drops more rapidly than L_vE. FCO_2 collapses in 4 min (including the time lag of 2 min), whereas L_vE requires 10–15 min to adapt to the new radiation regime. Also during the other two events, FCO_2 responds more rapidly to changes

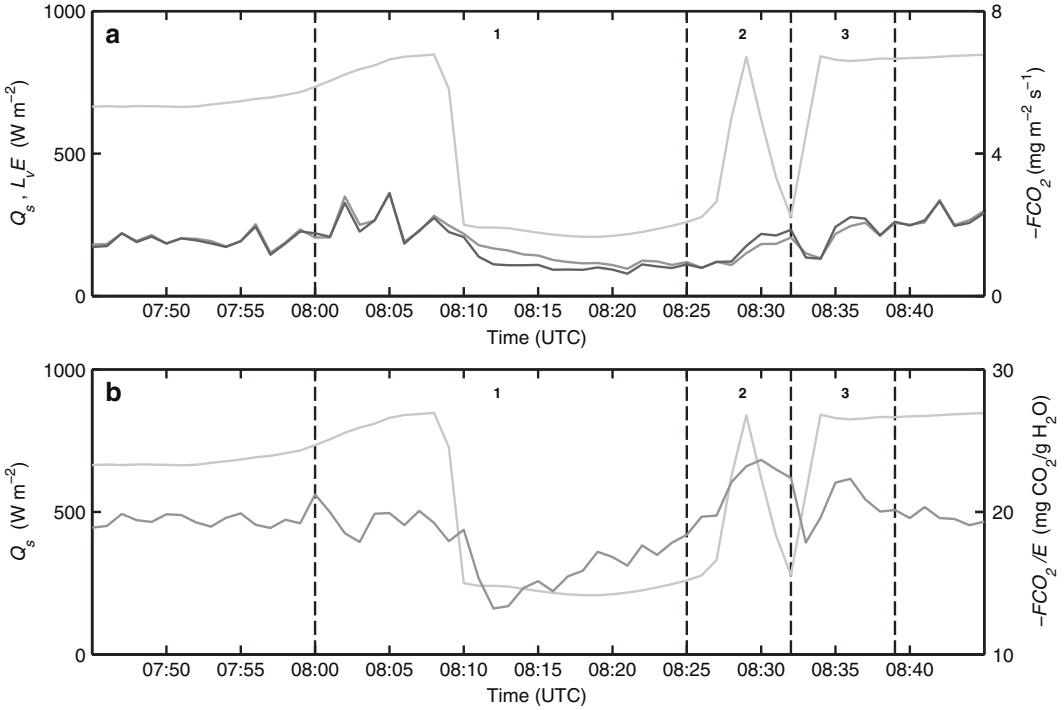

Fig. 10. Influence of varying incoming short-wave radiation on L_vE and FCO_2 for a situation on 5 June 2009 from 7:00 UTC to 10:30 UTC. (a) showing both L_vE and FCO_2 (b) showing the ratio of FCO_2 and E. In (a) Q_s is light grey, L_vE is grey, and $-FCO_2$ is dark grey. In (b) Q_s is light grey and $-FCO_2/E$ is grey.

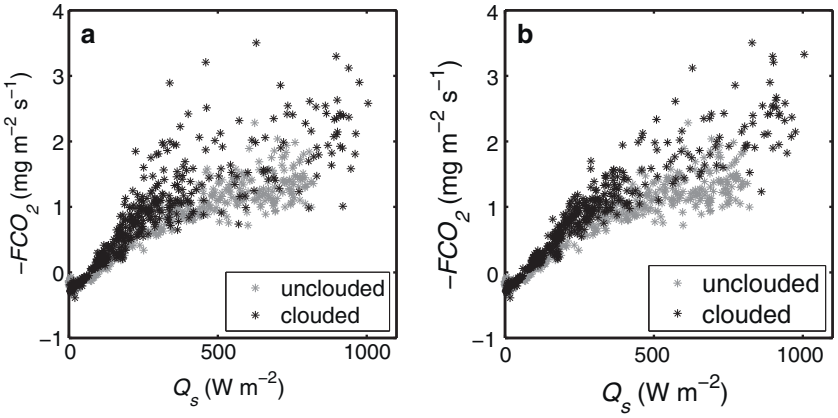

Fig. 11. Light–response curves for wheat on a cloudy morning (3 June 2009) and on a cloudless morning (1 June 2009), (a) without time-lag correction and (b) with time-lag correction.

in the radiation than does L_vE. This is confirmed by considering the ratio FCO_2/E in Fig. 10b. Throughout the selected period the ratio FCO_2/E fluctuates around 19 mg CO_2/g H_2O (cf. Baldocchi, 1994b) who found 11 mg CO_2/g H_2O), but when FCO_2 and L_vE respond to the changed radiative forcing the ratio clearly deviates from this mean (from 8:10 UTC onward). Hence, we conclude that the plant stomata did not cause the change in C_q^2 and $C_{qCO_2}^2$. Otherwise, both structure parameters would respond identically, as would the fluxes do. Determining the canopy resistance as described in Section 2.4 confirmed this conclusion, because the canopy resistance remained constant during all three events (not shown).

For FCO_2, these results are similar to Foken et al. (2001) over maize and Mauder et al. (2007) over cotton, who upon a solar eclipse estimated the delay of FCO_2 to be <5 min and <3 min, i.e. almost immediate.

For L_vE, our results are neither as long as the 25 min delay found by Foken et al. (2001), nor as short as the immediate response found by Mauder et al. (2007). First, there is a 2-min time lag, which is followed by a drop of L_vE in 3 min and accomplishes 67% of the total change in the flux. Finally, the response ends with a more gradual decrease of L_vE during the following 6–7 min. This brings the total response time at 11–12 min. For H a similar pattern as for L_vE is observed (not shown). This response time differs from Foken et al. (2001) who found a response time of 5 min, whereas it is more in agreement with the response time found by Mauder et al. (2007) of 8–13 min.

However, note that we do not expect identical response times. Firstly, in our case the radiation decreases in less than 2 min (causing a step response), whereas in case of the solar eclipses it takes about one to one-and-a-half hour to get a similar decrease (causing a sine response). Furthermore, the heat capacities of the systems differ, depending on the crop in question, development stage of the crops, atmospheric conditions, drought etc. In our case, there is an abrupt drop of Q_s. Nevertheless, storage changes of heat in the soil, in the wheat plants, and in the air, make that energy for H and L_vE remains available. Slowly, this energy is released (the surface temperature only slowly decreases), so that H and L_vE gradually decrease during the 5–12 min after the initial drop in Q_s.

Summarizing the above it is clear that solar radiation plays a more active role in determining FCO_2 than in determining L_vE. The photosynthesis rate, a bio-chemical rate, is directly affected by the solar radiation. As this rate determines the amount of CO_2 taken up by the plant, and with that FCO_2, there is a direct link between Q_s and FCO_2. For L_vE the link with Q_s is less direct, because L_vE is passively lost through the open plant stomata and also heat-storage changes affect L_vE.

Finally, we address the issue of the time lag (shift in time) that occurs between the radiation, and FCO_2 and L_vE respectively. The time lag is found by determining the optimal correlation between the radiation and the fluxes. Furthermore, it is identical for both FCO_2 and L_vE, and constant in time, but it differs per experiment (Transregio2009 vs. Transregio2008 or LITFASS2009). Especially the fact that we observe an increasing FCO_2 upon a decreasing solar radiation is giving confidence that we can exclude plant or soil effects. The invariableness of the 2-min time lag rather points to storage changes of CO_2 and water vapour in the lower two meters of the atmosphere between the (vegetation) surface and the sensor. For tall-tower observations, time lags are more familiar, but close to the surface (where the storage effect is very strong) this has gone unnoticed so far, because typically flux averages of 15–30 min are used instead of 1-min averages.

5.3. Light–response curves

Light–response or radiation–response curves are plots of Q_s with $-FCO_2$. They are a measure of how efficient plants can photosynthesise for a given light intensity. These curves differ among crops and depend on atmospheric conditions (Gilmanov et al., 2003; Kim and Verma, 1990; Moene and Van Dam, 2012; Nieveen et al., 1998). The advantage of determining these curves based on 1-min data is that only one morning is required to accurately determine a light response curve instead of one month. During one morning the development stage of the crop and atmospheric conditions are more constant than during one month and as such it becomes easier to study light response curves for specific conditions.

This is illustrated in Fig. 11. Fig. 11 shows the light–response curves based on 1-min measurements of FCO_2 for two mornings in June 2009 over wheat, i.e. a cloudless morning on 1 June 2009 from 3:15 UTC until 10:00 UTC and a cloudy morning on 3 June from 3:15 UTC until 10:30 UTC. On the cloudless day the temperature increased from 11 °C to 22 °C and the water-vapour deficit, *wvd*, increased from $wvd \approx 0$ hPa to $wvd \approx 10$ hPa, whereas on the cloudy day the temperature increased from 10 °C to 15 °C and *wvd* increased from $wvd \approx 0$ hPa to $wvd \approx 5$ hPa. As can be seen the light saturation is higher for the cloudy morning with the lower *wvd* (cf. Kim and Verma, 1990; Nieveen et al., 1998). This is related to the fact that the lower the *wvd* the better the water-use efficiency of crops (e.g. Baldocchi, 1994b; Nieveen, 1999). As L_vE had a similar magnitude on both days, and the water-use efficiency was higher on the cloudy day with the low *wvd*, the light saturation is higher for that day. Note, that a low *wvd* and cloudy conditions are closely related, because the temperature usually remains low during cloudy conditions. In addition, cloudy conditions benefit the light-use efficiency

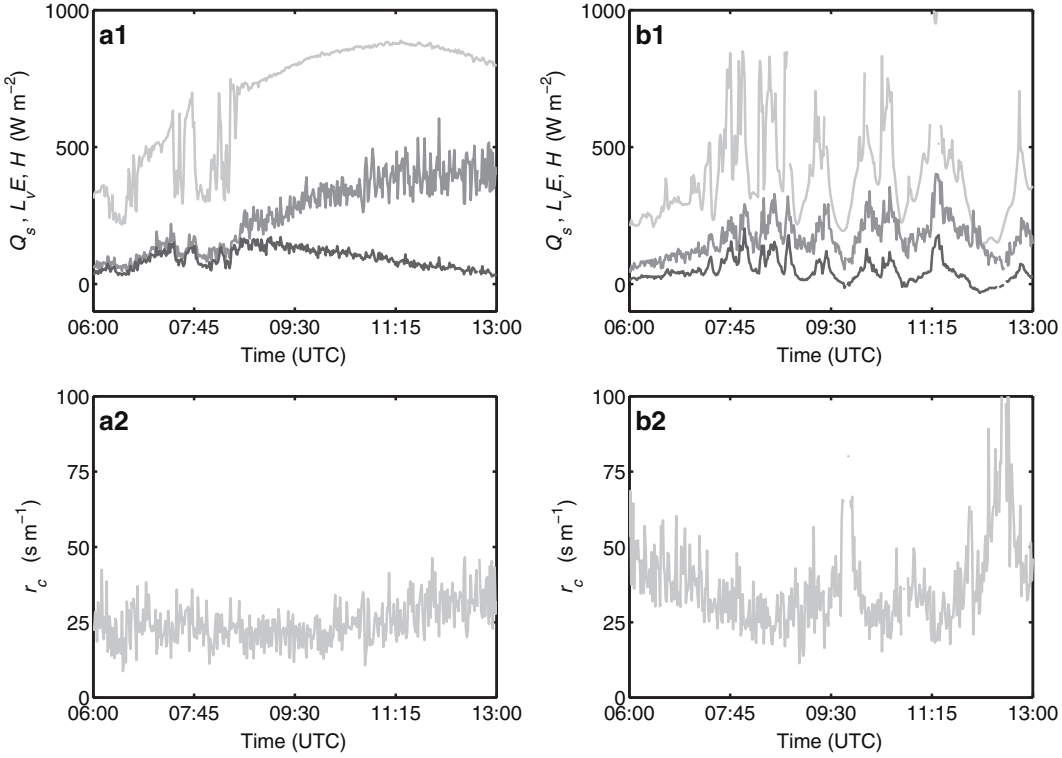

Fig. 12. 1-min values for the canopy resistance of wheat for (a) 2 June 2009 and (b) 4 June 2009. (a1) and (b1) show the incoming short-wave radiation, Q_s, together with the fluxes H and L_vE, (a2) and (b2) show the canopy resistance, r_c, for the corresponding time. In (a1) and (b1) Q_s is light grey, L_vE is grey and H is dark grey.

of vegetation, because there is more diffuse radiation than during unclouded conditions (Gu et al., 2002).

Another aspect that is shown by Fig. 11 is the importance of taking account the 2-min time lag of $-FCO_2$ compared to the radiation, i.e. plotting $Q_s(t)$ vs. $FCO_2(t+2)$. Fig. 11a shows the light–response curves for which the time lag has not been taken into account and Fig. 11b shows the light–response curves for which the time lag has been taken into account. Clearly, the scatter of the response curve from the cloudy situation is reduced by taking into account the time lag. Taking into account this time lag is not only relevant for working with 1-min fluxes, but also for determining light–response curves based on 30-min averaging intervals. For the cloudy conditions, the differences between $\overline{FCO_2(t)}^{30}$ and $\overline{FCO_2(t+2)}^{30}$ randomly varies between −3% and +7%.

5.4. Canopy resistance on 1-min time scales

This section discusses the results of the 1-min averaged canopy resistance. Fig. 12a1 and b1 show Q_s, together with L_vE and H, whereas Fig. 12a2 and b2 shows r_c. For this discussion, we selected two events. A day that was almost cloudless, 2 June 2009 (Fig. 12a) and a day that had a variable cloud cover, 4 June 2009 (Fig. 12b). To estimate r_c, we followed the procedure outlined in Section 2.4, using the resistance expressions for H and L_vE.

Starting with 2 June 2009, it can be seen that L_vE increases until 12:15 UTC and then slowly levels off, whereas H decreases from about 8:30 UTC. On the other hand, r_c is more or less constant. It fluctuates slightly during the clouded periods, reaches a minimum around 9:30 UTC and increases afterwards. Furthermore, r_c shows some noise, which is mainly caused by the noise in the L_vE measurements. These estimated values for r_c are slightly lower than found by Baldocchi (1994a), who found values typically between 50 and 100 s m^{-1}, and more comparable to Hatfield (1985) who found typical afternoon values of less than 30 s m^{-1} in the shade. However, r_c strongly depends on the atmospheric conditions, soil and crop properties such as the leaf-area index (Baldocchi, 1994a; Hatfield, 1985). Hence, we can safely assume that r_c is accurately resolved by this method.

Probably, r_c increases after 9:30 UTC, because plants reduce their stomatal aperture on large water loss (large L_vE) (Monteith, 1995; Mott and Parkhurst, 1991). The air gets drier and $wvd \approx 10$ hPa, corresponding to a relative humidity, RH, of about 50–60%. When plotting r_c against wvd a clear relation was observed (not shown), whereas no clear relation was observed between r_c and Q_s (not shown).

On the cloudy day both L_vE and H correlate well with Q_s. Note, that before 13:00 UTC H is negative for a while, which is a sign that warm air is advected. The response of r_c differs from that in the previous situation. First, r_c decreases and then from 9:30 UTC on r_c starts to fluctuate. The peaks in r_c coincide with dips in Q_s, albeit that the peaks lag approximately 5 min behind. Estimating the time between the base and top of the peaks leads to the conclusion that the wheat vegetation achieves the maximum change in r_c in about 20 min.

The question is whether wheat plants can physiologically control the flux by closing their stomata within such a time frame. Wheat belongs to the family of the Poaceae (grasses), which is characterized by its "dumb-bell-shaped" stomata (Franks and Farquhar, 2007; Hetherington and Woodward, 2003). Hetherington and Woodward (2003) state that because of the "dumb-bell design": "Smaller changes in guard and subsidiary cell turgor lead to greater increases in stomatal aperture (...). This efficiency and speed of stomatal opening in grasses enhances photosynthesis and water use efficiency compared with non-grass species." Furthermore, Franks and Farquhar (2007) conclude for wheat: "(...) the capability of very rapid stomatal movements (at a substantially faster rate than perhaps any other stomatal type) (...) may be explained by the unique morphology and mechanics of its dumb-bell-shaped stomata coupled with "see-sawing" of osmotic and turgor pressure

between guard and subsidiary cells during stomatal opening or closure". With "very rapid" they mean that the stomata can fully open within 4–9 min, depending on humidity (Franks and Farquhar, 2007).

Thus, we can conclude that indeed wheat is able to change its stomatal aperture on time intervals shorter than 20 min. However, stomatal response strongly depends on plant type and local circumstances such as water availability, heat, nutrient availability, competition with other plants, solar radiation, history, and time of the year. (Cardon et al., 1994). Most of these local circumstances are optimized for crops. In contrast to the situation in Fig. 12a, the air is more humid ($RH > 75\%$) during the situation in Fig. 12b and no clear relation between r_c and wvd is observed (not shown), whereas a relation between r_c and Q_s is clearly observed (not shown).

Finally, we want to mention that with the inverted Penman–Monteith method, by taking into account the time lags of H, L_vE, and G, we could reproduce r_c for the cloudy day, albeit with more scatter (not shown). During this day, $H(t+2)+L_vE(t+2)$ scattered around the 1:1 line when plotted against $Q_{net}(t)-G(t+4)$, indicating a closure of the energy balance. For the cloudless day, we could not reproduce these results, because $Q_{net}(t)-G(t+4) > H(t+2)+L_vE(t+2)$, i.e. the energy balance did not close. Non-closure of the energy balance occurs in many experiments, so great care must be taken when using the inverted Penman–Monteith Method. Thus, we conclude that through the resistance expressions for H and L_vE, the structure-parameter method most accurately solves 1-min averaged r_c and can be usefully applied to study vegetation responses in the field.

6. Conclusions

This paper discussed four combined methods for determining 1-min averaged L_vE and FCO_2 that can be used to evaluate L_vE under non-stationary conditions. The combined methods we discussed were the Bowen-variance method, the flux-variance method, the structure-parameter method, and the energy-balance method. The validation was based on the data from a wheat field near Merken (Germany), gathered in the framework of the Transregio32 experiment in 2009. Furthermore, an additional validation of the structure-parameter method was based on data from a wet sugar beet field near Merken gathered in the framework of Transregio32 in 2008 and data from a dry triticale field near Lindenberg (Germany) gathered in the framework of the LITFASS-2009 experiment.

The error analysis shows that the energy-balance method did not suffer from an averaging-time-dependent systematic error for 1-min averaging intervals, whereas the eddy-covariance method and flux-variance method have a large (−0.15) systematic error. Also the Bowen-variance method has a systematic error (+0.09), which results from a larger error in σ_T than in σ_q or σ_{qCO_2}. Finally, the structure-parameter method has a negligible systematic error in L_vE and FCO_2. The structure parameter is defined for separation distances that fall within the inertial sub-range of the scalar spectrum. Large eddies are not observed and do not need to be sampled. Consequently, structure-parameters are more robust statistical parameters than variances. In addition, the negligible systematic error in FCO_2, L_vE, H, and u_* confirms that the application of Monin–Obukhov similarity theory is justified for 1-min averaging intervals. Provided the conditions are homogeneous, the scintillometer yields a local flux estimate, which estimates the ensemble average by averaging in both space and time.

Similarly, we discussed the averaging-time-dependent random error in the combined methods. For 1-min averaging intervals, the random error of the combined methods is about half the random error of the eddy-covariance method. The exception is the energy-balance method. This method has a smaller error than the other combined methods, during the time of the day when the net radiation is dominant. For all combined methods holds that the combination of measuring H and u_* with the scintillometer and using standard deviations instead of covariances as scalar turbulence variables, greatly reduces the random error in the flux estimate.

Using Q_{net}, Q_s, and the Penman–Monteith model, we validated the combined methods and showed that the eddy-covariance method cannot resolve 1-min fluctuations in L_vE and FCO_2. Also the energy-balance method is unsuitable for measuring 1-min averaged fluxes. The assumption of a closed energy balance on H, L_vE, and G leads to a two-fold inaccuracy, because the non-closure is fully attributed to L_vE. Firstly, the energy-balance overestimates L_vE by about 20% and secondly, the phase of L_vE is biased to the phase of Q_{net}. In one case this even led to a negative L_vE estimate during daytime.

The three other combined methods are well able to resolve fluctuations in L_vE and FCO_2. Unfortunately, the Bowen-variance method has 30% less data than the other two combined methods, because data had to be omitted when $|r_{Tq}| < 0.2$ or $|\beta| < 0.1$ and $|r_{TqCO_2}| < 0.2$ or $|\alpha| < 1$. The flux-variance method resolved the fluctuations in the flux better than the Bowen-variance method, but the method suffers from its systematic error for 1-min averaging intervals. The structure-parameter method accurately estimates L_vE and FCO_2 for 1-min averaging intervals and was found to be the best and most robust method of all combined methods.

For a final, more extensive evaluation, we therefore applied the structure-parameter method to other experiments as well. It was shown that over sugar beets during wet conditions ($\beta \approx 0.2$), the method performed equally well in determining L_vE and FCO_2 as over the wheat field. During dryer conditions (β fluctuating between 0.3 and 2.5) L_vE did not correlate well with Q_{net}, because C_q^2 did not correlate with Q_{net}. L_vE was small and thus sensitive to disturbances. FCO_2, however, correlated as well with Q_s as during the other experiments and $C_{qCO_2}^2$ did do so as well.

Having finished the validation, we investigated the relevance of 1-min fluxes under non-stationary conditions, for several applications. First, we showed that the changes in the fluxes are not caused by changes in the turbulence, the transport mechanism, but by changes in the variations of the passive-scalar concentration, i.e. changes in the scalar concentration close to the vegetation.

Second, we showed that L_vE and FCO_2 respond differently to abrupt changes in solar radiation. Both fluxes lag 2 min behind the radiation, because of storage of water vapour and CO_2 in the air between the (vegetation) surface and our sensors. After these 2 min, FCO_2 almost immediately responds to a change in radiation, because the available radiation directly affects the chemical rate of photosynthesis and with that the CO_2 uptake. L_vE on the other hand shows a more dampened response, because stored (heat) energy still benefits L_vE (through the surface temperature) and the canopy resistance did not change. Therefore, L_vE (and H) change more gradually upon changes in the radiation than FCO_2. Of course, these findings depend strongly on the data set, because for the two other datasets, the time lag for example was found to be 1 min instead of 2 min.

Third, we studied light–response curves of the wheat canopy for a cloudy and unclouded morning and showed that the light-saturation level was significantly higher during the cloudy morning (as expected). This happened, because during the cloudy morning the water-vapour deficit was higher and with that the water-use efficiency. Furthermore, there was more diffuse radiation, all factors that benefit the light efficiency of the vegetation. In addition, we showed that especially during cloudy conditions it is crucial to

take into account the time lag between FCO_2 and Q_s. Even when determining curves based on 30-min Q_s and FCO_2 not taking into account the time lag can lead to errors that in our case randomly varied between −3% and +7%.

Fourth, we applied the structure-parameter method to study the 1-min averaged values of the canopy resistance. It was shown that via the resistance expressions for H and L_vE, the structure-parameter method accurately resolves 1-min r_c. Depending on the atmospheric conditions, r_c was driven by either the radiation or by the magnitude of L_vE (water-vapour deficit). Thus, it was shown that plants indeed modify their canopy resistance and thus modify turbulent fluxes on time intervals shorter than 30 min. We argued that for wheat plants this is easily possible, because they are able to adapt their stomatal apertures on time scales as short as 5 min. By taking into account the time lags in H, L_vE and G compared to Q_{net}, the inverted Penman–Monteith method could also be used to resolve 1-min r_c, but the accuracy of this method is very sensitive to non-closure of the energy balance.

Acknowledgements

The authors thank Alexander Graf from the Forschungszentrum Jülich for his great assistance during the field experiments in 2008 and 2009 and with the data processing. We also thank Frank Beyrich, Miranda Braam, and others from the German Weather Service (DWD) for their great assistance during the LITFASS-2009 experiment and subsequent data processing. Furthermore, the authors thank Arjan van Dijk for his work on this subject as presented in an internal report. Finally, the authors thank Bart Kruijt for a helpful discussion. This research was supported by the Dutch Technology Foundation (STW) under project number WTC7484.

References

Andreas, E.L., Fairall, C.W., Persson, P.O.G., Guest, P.S., 2003. Probability distributions for the inner scale and the refractive index structure parameter and their implications for flux averaging. J. Appl. Meteorol. 42 (9), 1316–1329.

Andreas, E.L., Hill, R.J., Gosz, J.R., Moore, D.I., Otto, W.D., Sarma, A.D., 1998. Statistics of surface-layer turbulence over terrain with metre-scale heterogeneity. Boundary-Layer Meteorol. 86 (3), 379–408.

Baldocchi, D., 1994a. A comparative-study of mass and energy-exchange over a closed C-3 (wheat) and an open C-4 (corn) canopy. 1. The partitioning of available energy into latent and sensible heat-exchange. Agric. Forest Meteorol. 67 (3–4), 191–220.

Baldocchi, D., 1994b. A comparative-study of mass and energy-exchange rates over a closed C-3 (wheat) and an open C-4 (corn) crop. 2. CO_2 exchange and water-use efficiency. Agric. Forest Meteorol. 67 (3–4), 291–321.

Baldocchi, D.D., 2003. Assessing the eddy covariance technique for evaluating carbon dioxide exchange rates of ecosystems: past, present and future. Global Change Biol. 9 (4), 479–492.

Bastiaanssen, W.G.M., Pelgrum, H., Droogers, P., De Bruin, H.A.R., Menenti, M., 1997. Area-average estimates of evaporation, wetness indicators and top soil moisture during two golden days in EFEDA. Agric. Forest Meteorol. 87 (2–3), 119–137.

Beyrich, F., Bange, J., Hartogensis, O.K., Raasch, S., Braam, M., van Dinther, D., Gräf, D., Van Kesteren, B., Van den Kroonenberg, A.C., Maronga, B., Martin, S., Moene, A.F., 2012. Towards a validation of scintillometer measurements: the LITFASS-2009 experiment. Boundary-Layer Meteorol. 144 (1), 83–112.

Businger, J.A., Wyngaard, J.C., Izumi, Y., Bradley, E.F., 1971. Flux–profile relationships in the atmospheric surface layer. J. Atmos. Sci. 28 (2), 181–189.

Cardon, Z.G., Berry, J.A., Woodrow, I.E., 1994. Dependence of the extent and direction of average stomatal response in *Zea-Mays* L and *Phaseolus-Vulgaris* L on the frequency of fluctuations in environmental stimuli. Plant Physiol. 105 (3), 1007–1013.

Cheinet, S., Siebesma, A.P., 2009. Variability of local structure parameters in the convective boundary layer. J. Atmos. Sci. 66 (4), 1002–1017.

Chen, J.M., Zhang, R.H., 1989. Studies on the measurements of crop emissivity and sky temperature. Agric. Forest Meteorol. 49 (1), 23–34.

De Bruin, H.A.R., 1987. From Penman to Makkink. Proceedings & Information - Committee for Hydrological Research TNO 39, 5–30.

De Bruin, H.A.R., Jacobs, C.M.J., 1993. Impact of CO_2 enrichment on the regional evapotranspiration of agro-ecosystems, a theoretical and numerical modelling study. Vegetatio 104–105 (1), 307–318.

De Bruin, H.A.R., Van Den Hurk, B.J.J.M., Kroon, L.J.M., 1999. On the temperature–humidity correlation and similarity. Boundary-Layer Meteorol. 93 (3), 453–468.

De Bruin, H.A.R., Verhoef, A., 1999. Reply to the comments on 'a new method to determine the zero-plane displacement', by Zhang and Park. Boundary-Layer Meteorol. 91 (1), 141–143.

De Bruin, H.A.R., Meijninger, W.M.L., Smedman, A.S., Magnusson, M., 2002. Displaced-beam small aperture scintillometer test. Part I: The wintex data-set. Boundary-Layer Meteorol. 105 (1), 129–148.

de Rooy, W.C., Holtslag, A.A.M., 1999. Estimation of surface radiation and energy flux densities from single-level weather data. J. Appl. Meteorol. 38 (5), 526–540.

Evans, J.G., 2009. Long-path scintillometry over complex terrain to determine areal-averaged sensible and latent heat fluxes. Ph.D. Thesis. The University of Reading, Reading, 201 pp.

Foken, T., Wichura, B., Klemm, O., Gerchau, J., Winterhalter, M., Weidinger, T., 2001. Micrometeorological measurements during the total solar eclipse of August 11, 1999. Meteorol. Z. 10 (3), 171–178.

Foken, T., Wimmer, F., Mauder, M., Thomas, C., Liebethal, C., 2006. Some aspects of the energy balance closure problem. Atmos. Chem. Phys. 6, 4395–4402.

Franks, P.J., Farquhar, G.D., 2007. The mechanical diversity of stomata and its significance in gas-exchange control. Plant Physiol. 143 (1), 78–87.

Gilmanov, T.G., Verma, S.B., Sims, P.L., Meyers, T.P., Bradford, J.A., Burba, G.G., Suyker, A.E., 2003. Gross primary production and light response parameters of four Southern Plains ecosystems estimated using long-term CO_2-flux tower measurements. Global Biogeochem. Cy. 17 (2), 1071, http://dx.doi.org/10.1029/2002GB002023.

Graf, A., Schuttemeyer, D., Geiss, H., Knaps, A., Mollmann-Coers, M., Schween, J.H., Kollet, S., Neininger, B., Herbst, M., Vereecken, H., 2010. Boundedness of turbulent temperature probability distributions, and their relation to the vertical profile in the convective boundary layer. Boundary-Layer Meteorol. 134 (3), 459–486.

Green, A.E., Astill, M.S., McAneney, K.J., Nieveen, J.P., 2001. Path-averaged surface fluxes determined from infrared and microwave scintillometers. Agric. Forest Meteorol. 109 (3), 233–247.

Green, A.E., McAneney, K.J., Astill, M.S., 1994. Surface-layer scintillation measurements of daytime sensible heat and momentum fluxes. Boundary-Layer Meteorol. 68 (4), 357–373.

Gu, L.H., Baldocchi, D., Verma, S.B., Black, T.A., Vesala, T., Falge, E.M., Dowty, P.R., 2002. Advantages of diffuse radiation for terrestrial ecosystem productivity. J. Geophys. Res. 107 (D5–6), 4050, http://dx.doi.org/10.1029/2001jd001242.

Hartogensis, O.K., De Bruin, H.A.R., Van de Wiel, B.J.H., 2002. Displaced-beam small aperture scintillometer test. Part II: CASES-99 stable boundary-layer experiment. Boundary-Layer Meteorol. 105 (1), 149–176.

Hatfield, J.L., 1985. Wheat canopy resistance determined by energy-balance techniques. Agron. J. 77 (2), 279–283.

Hetherington, A.M., Woodward, F.I., 2003. The role of stomata in sensing and driving environmental change. Nature 424 (6951), 901–908.

Huband, N.D.S., Monteith, J.L., 1986. Radiative surface-temperature and energy-balance of a wheat canopy. 1. Comparison of radiative and aerodynamic canopy temperature. Boundary-Layer Meteorol. 36 (1–2), 1–17.

Kelliher, F.M., Leuning, R., Raupach, M.R., Schulze, E.D., 1995. Maximum conductances for evaporation from global vegetation types. Agric. Forest Meteorol. 73 (1–2), 1–16.

Kim, J., Verma, S.B., 1990. Carbon-dioxide exchange in a temperate grassland ecosystem. Boundary-Layer Meteorol. 52 (1–2), 135–149.

Lenschow, D.H., Mann, J., Kristensen, L., 1994. How long is long enough when measuring fluxes and other turbulence statistics. J. Atmos. Ocean. Tech. 11 (3), 661–673.

Mahrt, L., 2010. Computing turbulent fluxes near the surface: needed improvements. Agric. Forest Meteorol. 150 (4), 501–509.

Mauder, M., Desjardins, R.L., Oncley, S.P., MacPherson, I., 2007. Atmospheric response to a partial solar eclipse over a cotton field in central California. J. Appl. Meteorol. Clim. 46 (11), 1792–1803.

Meijninger, W.M.L., Beyrich, F., Lüdi, A., Kohsiek, W., De Bruin, H.A.R., 2006. Scintillometer-based turbulent fluxes of sensible and latent heat over a heterogeneous land surface – a contribution to LITFASS-2003. Boundary-Layer Meteorol. 121 (1), 89–110.

Moene, A.F., Schüttemeyer, D., 2008. The effect of surface heterogeneity on the temperature–humidity correlation and the relative transport efficiency. Boundary-Layer Meteorol. 129 (1), 99–113.

Moene, A.F., Van Dam, J.C., 2012. Transport Processes in the Atmosphere–Vegetation–Soil Continuum. Cambridge University Press, Cambridge, UK, in preparation.

Monteith, J.L., 1965. Evaporation and environment. Symp. Soc. Exp. Biol. 19, 205–234.

Monteith, J.L., 1995. A reinterpretation of stomatal responses to humidity. Plant Cell Environ. 18 (4), 357–364.

Mott, K.A., Parkhurst, D.F., 1991. Stomatal responses to humidity in air and helox. Plant Cell Environ. 14 (5), 509–515.

Nieveen, J.P., 1999. Eddy Covariance and Scintillation Measurements of Atmospheric Exchange Processes over Different Types of Vegetation. Wageningen University, Wageningen, The Netherlands, 121 pp.

Nieveen, J.P., Jacobs, C.M.J., Jacobs, A.F.G., 1998. Diurnal and seasonal variation of carbon dioxide exchange from a former true raised bog. Global Change Biol. 4 (8), 823–833.

Oncley, S.P., Friehe, C.A., Larue, J.C., Businger, J.A., Itsweire, E.C., Chang, S.S., 1996. Surface-layer fluxes, profiles, and turbulence measurements over uniform terrain under near-neutral conditions. J. Atmos. Sci. 53 (7), 1029–1044.

Papaioannou, G., Papanikolaou, N., Retalis, D., 1993. Relationships of photosynthetically active radiation and shortwave irradiance. Theor. Appl. Climatol. 48 (1), 23–27.
Paulson, C.A., 1970. The mathematical representation of wind speed and temperature profiles in the unstable atmospheric surface layer. J. Appl. Meteorol. 9 (6), 857–861.
Priestley, C.H.B., Taylor, R.J., 1972. On the assessment of surface heat flux and evaporation using large-scale parameters. Monthly Weather Review 100, 81–92.
Scanlon, T.M., Kustas, W.P., 2010. Partitioning carbon dioxide and water vapor fluxes using correlation analysis. Agric. Forest Meteorol. 150 (1), 89–99.
Schotanus, P., Nieuwstadt, F.T.M., De Bruin, H.A.R., 1983. Temperature measurement with a sonic anemometer and its application to heat and moisture fluxes. Boundary-Layer Meteorol. 26 (1), 81–93.
Shuttleworth, W.J., 2007. Putting the 'vap' into evaporation. Hydrol. Earth Syst. Sci. 11 (1), 210–244.
Stull, R.B., 1988. An Introduction to Boundary Layer Meteorology. Kluwer Academic Publishers, Dordrecht, The Netherlands, 666 pp.
Sun, X., Zhu, Z., Xu, J., Yuan, G., Zhou, Y., Zhang, R., 2005. Determination of averaging period parameter and its effects analysis for eddy covariance measurements. Science in China, Series D: Earth Sciences 48 (Suppl. 1), 33–41.
Tatarskii, V.I., 1961. Wave Propagation in a Turbulent Medium. McGraw-Hill Book Company Inc, New York, USA, 285 pp.
Thiermann, V., Grassl, H., 1992. The measurement of turbulent surface-layer fluxes by use of bichromatic scintillation. Boundary-Layer Meteorol. 58 (4), 367–389.
Van Dijk, A., Moene, A.F., De Bruin, H.A.R., 2004. The Principles of Surface Flux Physics: Theory, Practice and Description of the ECPACK Library. Meteorology and Air Quality Group, Wageningen University, Wageningen.
van Dinther, D., 2009. Obtaining Reliable H_2O and CO_2 Fluxes using Scintillometry Combined with Scalar Turbulence Measurements. Wageningen University, Wageningen, 86 pp.
Van Kesteren, B., 2012. Measuring water-vapour and carbon-dioxide fluxes at field scales with scintillometry. Ph.D. Thesis. Wageningen University, Wageningen, 220 pp.
Van Kesteren, B., Hartogensis, O.K., van Dinther, D., Moene, A.F., De Bruin, H.A.R., 2012. Measuring H_2O and CO_2 fluxes at field scales with scintillometry: Part I – Introduction and validation of four methods. Agric. Forest Meteorol., http://dx.doi.org/10.1016/j.agrformet.2012.09.013.
Wittich, K.P., 1997. Some simple relationships between land-surface emissivity, greenness and the plant cover fraction for use in satellite remote sensing. Int. J. Biometeorol. 41 (2), 58–64.
Wolf, A., Saliendra, N., Akshalov, K., Johnson, D.A., Laca, E., 2008. Effects of different eddy covariance correction schemes on a energy balance closure and comparisons with the modified Bowen ratio system. Agric. Forest Meteorol. 148 (6–7), 942–952.
Wyngaard, J.C., Clifford, S.F., 1978. Estimating momentum, heat and moisture fluxes from structure parameters. J. Atmos. Sci. 35 (7), 1204–1211.
Zeiger, E., Farquhar, G.D., Cowan, I.R., 1987. Stomatal Function. Stanford University Press, Stanford, Calif., USA, xiv, 503 p.